Journal of Heat and Mass Transfer Research

Journal homepage: https://jhmtr.semnan.ac.ir

Semnan University

ISSN: 2383-3068

Review Article

Gas Cyclone Performance Prediction: A State-of-the-Art Review of Theoretical Modeling Approaches

Farzad Parvaz [a] *, Masoud Dorfeshan [b], Sadegh Nikbakht Naserabad [c]

[a] *Department of Mechanical Engineering, Semnan University, P. O. Box 35131-191, Semnan, Iran*

[b] *Behbahan Khatam Alanbia University of Technology, Department of Mechanical Engineering, Faculty of Engineering, Behbahan, Iran*

[c] *Energy Engineering Department, Faculty of Gas & Petroleum, Yasouj University, Gachsaran, Iran*

ARTICLE INFO

Article history:

Received: 2025-03-17

Revised: 2025-09-08

Accepted: 2025-10-26

Keywords:

Gas cyclone approaches,
Pressure drop,
Collection efficiency,
Particle flow,
Flow pattern

ABSTRACT

Existing investigations present numerous theoretical frameworks for analyzing conventional gas cyclones, focusing on key performance indicators (KPIs) such as inlet velocities, pressure drop, and collection efficiency. These KPIs are critical in industries where understanding the transport and behavior of solid particles is paramount. Traditionally, predicting the complex swirling gas flow within these cyclones has relied on empirical studies, which are both resource-intensive and time-consuming. While theoretical models offer a potentially more efficient and cost-effective approach, they have received comparatively less attention in previous investigations of overall gas cyclone performance. This research endeavors to rigorously evaluate the accuracy of established gas separator theories. The methodology involves comparing theoretical predictions with numerical simulations and experimental data obtained at a controlled solid loading rate of 1 g/m^3, across velocities of 5 and 10 m/s. A notable consensus emerged, favoring Muschelknautz's approach for predicting collection efficiency. Similarly, the Lapple and Shepherd model demonstrated utility in estimating pressure drop under conditions of low solid loading. However, several scholars have highlighted discrepancies arising from the influence of wall friction within gas cyclones and a general insensitivity to the particle phase within these models. This section provides an overview of published CFD simulation studies on cyclones, specifically examining the effects of high particle loading, at room and at high temperatures. Furthermore, the Mothes and Löffler model was identified as capable of accurately predicting the natural vortex length, a critical parameter for the design and optimization of conventional gas cyclones.

1. Introduction

In 1885, John M. Finch of the United States received the first patent for a cyclone separator, assigned to the Knickerbocker Company. Although this early device, then termed a "dust collector," incorporated the core functional elements of contemporary cyclone designs (see Fig. 1), its distinguishing feature was the lateral discharge of collected dust from the cylindrical body, as opposed to the now-standard conical bottom outlet. Gas cyclones are favored in industries involving particle transport due to their low maintenance costs, capacity to remove larger particles, affordability, and resilience to harsh environmental conditions. Gas cyclones are

* **Corresponding author.**
E-mail address: *f.parvaz1986@gmail.com*

Cite this article as:
Parvaz, F., Nikbakht Naserabad, S., Dorfeshan, M., 2026. Gas Cyclone Performance Prediction: A State-of-the-Art Review of Theoretical Modeling Approaches. *Journal of Heat and Mass Transfer Research*, 13(1), pp. 43-72.
https://doi.org/10.22075/JHMTR.2025.37145.1693

utilized to separate gas mixtures containing water or oil particles and droplets, adapting to various industrial process needs. Gas-particle cyclones rely on the tangential injection of a non-uniform particle stream into a cylindrical separation chamber. Particle trajectories are then dictated by the boundary conditions at the cyclone walls, which are typically characterized by a rebound effect. The interplay of lift forces and the gaseous boundary layer near the walls further separates fine particles (directed to the outlet pipe) from denser particles (directed towards the bottom of the cyclone). Gas-oil cyclones exhibit a modified separation mechanism, where the density difference between oil and water governs droplet behavior. In this scenario, the impact of oil droplets on the cyclone walls results in the formation of a liquid film, influencing the rebound dynamics [1]. The contrasting behaviors of solid particles and liquid droplets in these cyclone configurations are illustrated in Figure 2.

Ongoing numerical and experimental studies by various researchers have aimed to enhance gas cyclone performance [4,5, 6, 7–12, 13–22, 23–32, 33,34]. In terms of numerical investigations, Fu et al. [35] have carried out a study of the effects of a helical baffle on gas-oil separation. They have observed that the helical guide vane serves to enlarge the separator wall surface area, which enhances droplet-wall contact and improves the collection efficiency, particularly for smaller droplets. This design is especially suited for use downstream of a condensing tank to capture any remaining entrained droplets.

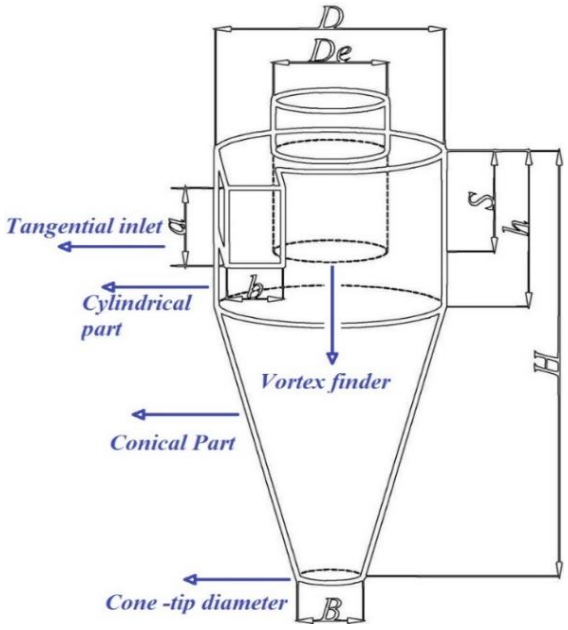

Fig. 1. Gas cyclone schematic

Dai et al. [36] investigated liquid film behavior within a micro-cyclone separator designed for hydrogen fuel cells using a combined Eulerian Wall Film (EWF) and Volume of Fluid (VOF) modeling strategy. They recognized that the precision of the simulations could be affected by an excessively thick liquid film. To address this, they initially modeled the liquid film using the EWF method, transitioning to a VOF-based representation once the film thickness reached a predetermined level. This approach emphasizes the critical role of accurate and adaptive modeling in improving the performance of gas-liquid separation systems. Gao et al. [37] have studied the impact of a spiral guide on an FCC gas cyclone. They reported that in contrast to cyclone separators equipped with a vortex finder, those without one experience a significant increase in short-circuit flow and greater vortex core instability. This leads to increased particle escape via the short-circuit flow path and heightened particle backmixing at the wall, which negatively impacts separation efficiency.

Separators incorporating guide vanes, however, exhibit a different behavior. The spiral channel in these designs promotes particle pre-separation, causing particles to concentrate towards the cylinder wall. Despite the increase in short-circuit flow, the particle escape and wall backmixing are lower than in the baseline PV design, resulting in improved separation. Sun et al. [38] investigated a cyclone separator design featuring a secondary cleaning gas injection system.

Their findings indicated that strategic selection of flow channel width and extension length allowed the cleaning gas to reduce total deposited particle mass by more than 60%. Despite this improvement in separation performance, the implementation of a secondary cleaning gas stream necessitates an external air supply, resulting in increased energy consumption. Moreover, the injection system is prone to clogging issues over extended periods of operation. Barua et al. [39] have performed a study of the effect of inlet width and height variation on a multi-channel gas cyclone. Their obtained results revealed that the effect of axial velocity on collection efficiency in cyclone separators is complex. While higher downward axial velocities generally enhance particle collection, the presence of significant short-circuit flow can disrupt the intended vortex pattern. This disruption leads to a reduction in axial velocity and, consequently, a decline in the overall separation performance of the cyclone.

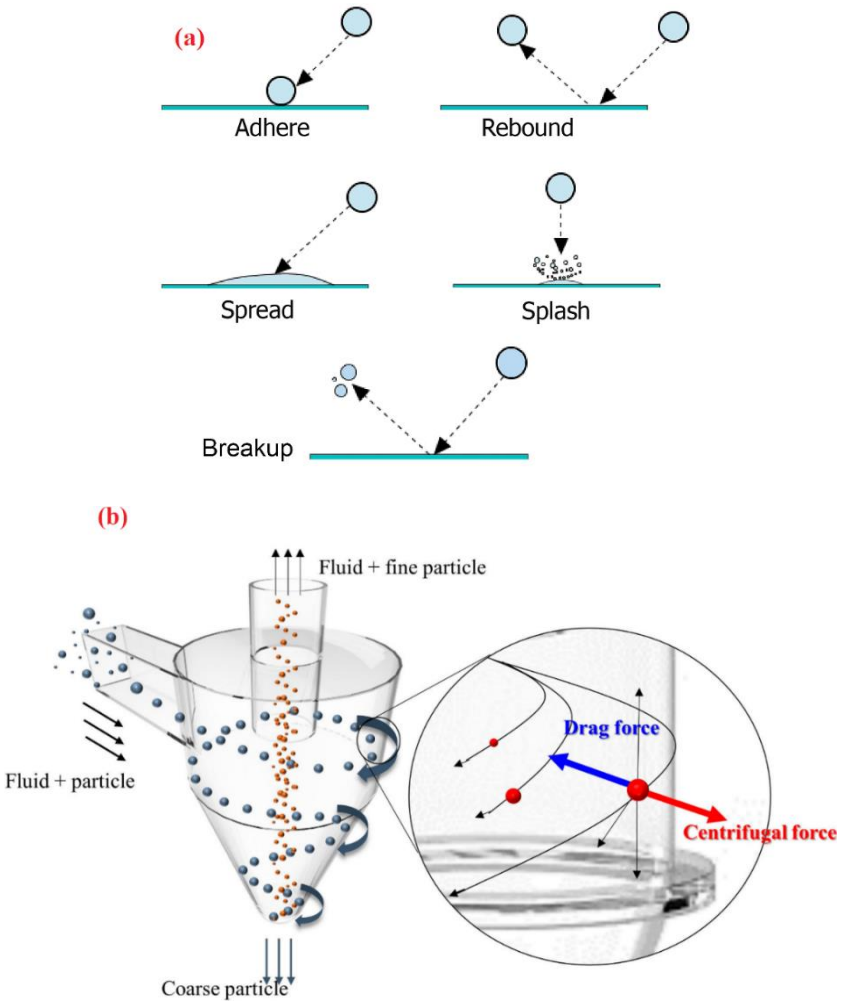

Fig. 2. Movement of droplets[2] and particle[3] with wall

Madaliev et al. [40] have numerically investigated the hydrodynamics of a centrifugal gas cyclone. They observed that the implementation of a screw cyclone, and in particular a screw cyclone with a variable pitch screw, leads to a notable increase in the efficient collection of zinc particles. Samadi et al. [41] have studied the use of compact gas cyclones to classify solid particles. Their results indicated that complete separation of particles with a diameter of six microns or greater is achieved, with a cut point diameter of 1 μm. To further understand the performance of the introduced cyclone design, numerical simulations were conducted to analyze the gas flow characteristics and visualize the trajectories of particles within the system. Tang et al. [42] conducted a study of a downhole spiral cyclone to separate natural gas hydrate. They observed that the separator design was optimized with the following structural parameters: a vortex guide plate positioned at 28 mm, 6 inlets, a circular cross-sectional geometry for the spiral flow channel, 2 spiral lines, and an overflow pipe depth of 100 mm. Sun et al. [43] simulated an elliptical gas cyclone. They found that an elliptical cross section inside a gas cyclone can increase by 2% collection efficiency and reduce by 43% pressure loss. Zhao et al. [44] have investigated the effect of local erosion on rotating particles and flow patterns. They observed that the flow field complexity within a cyclone separator is increased by localized wear and deformation, as these irregularities generate local vortices. As the erosion thickness increases, the vortex core exhibits amplified oscillations, resulting in greater particle entrainment within the ash hopper. Moreover, the localized wall wear disrupts the intended particle pathways, causing a significant number of particles to overcome centrifugal forces and migrate radially. The cumulative effect of localized wear and deformation is a substantial reduction in the separation efficiency of the cyclone separator. Employing a combined computational fluid dynamics and discrete element method (CFD-DEM) simulation approach, Liang et al. [45] examined the impact of operating conditions on particle rotation within a cyclone separator. Their findings indicated that particle rotation and revolution velocities decreased as both particle size and feed rate increased.

In terms of theoretical investigations, these efforts often involve theoretical designs to predict collection efficiency and pressure drop. Most theoretical models share common assumptions, including: 1) particles are spherical; 2) particle interactions are negligible; 3) radial gas velocity is zero; and 4) Stokes' law governs radial force on particles [46]. Theoretical forecasting of gas cyclone performance is crucial for gas separator design and setting performance targets. While these theories are all built on the aforementioned hypotheses, their validity is also dependent on turbulent flow assumptions within the separator, as well as specific operational or geometric conditions. Therefore, the reliability of a selected theory is judged against numerical or experimental findings. Comparisons, however, remain relatively uncommon in industrial practice and subsequent investigations. Moreover, existing theories that assess pressure drop and collection efficiency are primarily grounded in the turbulent flow characteristics of industrial-scale gas cyclones, often failing to accurately predict the performance of smaller gas cyclones [47].

In the current study, frequently applied theories were selected based on numerical and experimental data concerning turbulence within industrial-scale gas cyclones, as obtained by Leung and Bogodage [48,49]. Data included a solid loading rate of 1 g/m^3 at two tangential inlets with velocities of 5 and 10 m/s. Bogodage and Leung [49] also utilized numerical data from simulations conducted under the same experimental conditions, employing Large Eddy Simulation (LES) with a one-way coupling assumption to model two-phase flow and particle behavior in a gas stream. However, it's worth noting that many existing gas cyclone theories are based on separators with different inlet designs, such as slotted and circular inlets, unlike the rectangular inlet (similar in cross-sectional area) used by Leung and Bogodage [49]. The objective of this investigation is to review conventional gas cyclone theories and employ experimental data to identify suitable and useful approaches for predicting pressure drop and collection efficiency. Furthermore, drawing on conventional gas cyclone theories, Bogodage [49] analyzed numerical data related to velocity profiles, including tangential, axial, and radial velocities. The primary objective of this work is to review recent developments in the modeling and characterization of gas-particle separation dynamics within cyclone separators. The review specifically examines various modeling approaches used to simulate flow patterns, pressure drop, gas-particle separation behaviors (particle cut-size and grade efficiency), and the operation of dense medium cyclones. A comprehensive evaluation of the accuracy, applicability, and limitations of these models is presented. The review concludes by outlining prospective avenues for future advancements in the modeling of gas-particle cyclonic separation.

2. Collection Efficiency

While an understanding of cyclone flow is essential, it only provides a partial picture of how these devices accomplish their primary function: the removal of solid particles from dust-laden gas streams. The collection of particles within a cyclone is ultimately determined by the resultant of forces acting on the particles, causing them to migrate to the cyclone walls. Although centrifugal, drag, and gravitational forces are commonly considered, other potentially influential factors, such as particle-particle and particle-wall interactions, are often overlooked despite their potential impact on the collection process. The ability of a cyclone separator to remove particles is quantified by its collection efficiency, Z, defined as the proportion of the incoming solids flow rate that is successfully separated. Since cyclones often handle particles with a broad distribution of sizes, it is common to consider size-dependent efficiencies. In the limit where particle size intervals become infinitesimally small, a continuous function Z(x) is obtained, representing the grade-efficiency or fractional efficiency of the cyclone for particles of size x. A detailed mathematical treatment of the relationship between Z(x) and Z can be found in Ref. [46]. In the following discussion, we will focus on the converse relationship: given that f(x) represents the particle size distribution (PSD) at the inlet of the cyclone:

$$\eta = \int_0^\infty f(x)\eta(x)dx \tag{1}$$

The grade-efficiency curve offers a more accurate assessment of the inherent separation capabilities of a cyclone separator. This is because, by definition, it is solely a function of the cyclone's design and operating parameters and is independent of the particle size distribution (PSD) at the inlet. On the other hand, the total collection efficiency, as shown in Eq. (1), depends on both the characteristics of the cyclone and the inlet PSD, making it a less intrinsic measure of the apparatus's performance. The inherent behavior of cyclone separators dictates that very large particles will be consistently separated from the gas stream, while very fine particles will inevitably escape collection. In an idealized scenario characterized by laminar and fully ordered flow, a distinct cutoff point would exist at a specific particle size $\eta(x)$, representing the threshold above which particles are separated and below which they are not. However, given that real-

world flow conditions are far from ideal (and fixed particles cannot be separated or escape collection), particles of a certain size will have a range of likely separation. The 50% point for the cut size would be the ideal metric with a probability close to 0 and less than 1, where $\eta(x_{50}) = 0.5$. A schematic depiction of key definitions related to cyclone collection efficiency is provided in Figure 3. For example, the horizontal cross-section of a cyclone separator in Figure 4 helps define the volume of gas and particles. If all particles have the same unit volume C then they can be mapped as a function of radius r and phase angle θ. The current model suggests that a radius dr has direct contact with the wall where they can accumulate. These particles will flow from distances rdθ in the angular direction and distances dz in the vertical direction.

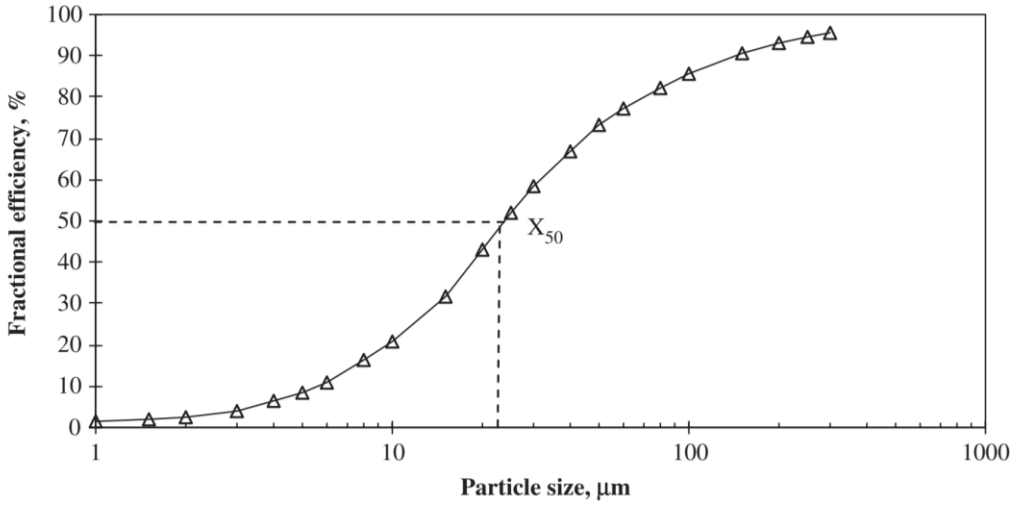

Fig. 3. Experimentally-derived fractional efficiency curve [50]

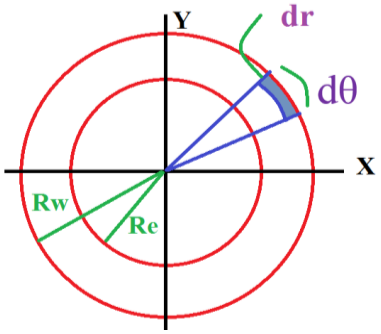

Fig. 4. Schematic representation of the gas-particle separation process within a cyclone cross-section

Therefore, the total number of particles collected within the defined control volume can be expressed as:

$$\begin{aligned} -dN &= C(R_w,\theta)(R_w - dr)drdzd\theta \\ &= C(R_w,\theta)R_w drdzd\theta - C(R_w,\theta)d\theta dz(dr)^2 \\ &\approx C(R_w,\theta)R_w drdzd\theta \end{aligned} \quad (2)$$

Considering all particle sizes, the total number of particles present within the control volume is:

$$N = \int_{R_e}^{R_w} \left[C(r,\theta) rd\theta dz \right] dr \quad (3)$$

Based on boundary layer separation theory, the proportion of particles removed within the control volume can be determined by combining Eq. (2) and Eq. (3):

$$-\frac{dN}{N} = \frac{C(R_w,\theta)R_w dr}{\int_{R_e}^{R_w} C(r,\theta) rdr} \quad (4)$$

The trajectory equation close to the wall is given as:

$$\frac{dr}{d\theta} = \left(\frac{\rho_p d_p^2 C_c}{18\mu_g} \right) V_{\theta w} \quad (5)$$

By combining and integrating the preceding equation, one obtains:

$$\frac{dr}{d\theta} = \left(\frac{\rho_p d_p^2 C_c}{18\mu_g} \right) V_{\theta w} \frac{C(R_w,\theta)R_w dr}{\int_{R_e}^{R_w} C(r,\theta) rdr} \quad (6)$$

The grade efficiency is therefore:

$$\begin{aligned} \eta_i &= 1 - \frac{N}{N_0} \\ &= 1 - \exp\left(-\left(\frac{\rho_p d_p^2 C_c}{18\mu_g} \right) V_{\theta w} \frac{C(R_w,\theta)R_w dr}{\int_{R_e}^{R_w} C(r,\theta) rdr} \right) \end{aligned} \quad (7)$$

According to Li and Wang [51], θT is defined as:

$$\theta_T = \frac{2\pi(S+L)}{a} \tag{8}$$

$$L = 2.3D_e\left(\frac{D^2}{ab}\right)^{1/3} for L \le H-h \tag{9}$$

$$\begin{matrix} L \succ H-h \\ for \\ L = H-S \end{matrix} \tag{10}$$

Table 1 lists a range of theoretical models utilized to evaluate the collection efficiency of gas cyclones, as identified in the existing literature. A concise overview of these models is provided in the subsequent sections.

Table 1. Overview of theoretical correlations for collection efficiency

Model	**Equations**				
Lapple	$d_{50} = \sqrt{\frac{9\mu b}{2\pi\rho_p v_{in} N}}$	(11)	$\eta_x = \frac{1}{1+\left(\frac{d_{50}}{d_x}\right)^2}$	Suggested by Theodore and Paola [52]	(12)
	$d_{50} = \sqrt{\frac{9\mu Q}{\pi\rho_p v_{\theta cs}^2 h^*}}$	(13)			
Bart	$h^* = \begin{cases} H-S\,(if D_e \langle B) \\ \frac{(H-h)(D-D_e)}{(D-B)} + (h-S)\,(if D_e \langle B) \end{cases}$	(14)	$v_{\theta CS} = v_x\left(\frac{0.5\pi D_e(D-b)}{2ab\alpha + h^*(D-b)f\,\pi}\right)$		(15)
	$\alpha = 1-1.2\left(\frac{b}{D}\right)$	(16)	$\eta_x = \frac{1}{1+\left(\frac{U_{ts}}{U_{ts}^*}\right)^{-3.2}}$		(17)
	$U_{ts}^* = \frac{Qg}{2\pi h^* v_{\theta CS}^2}$	(18)	$\frac{U_{ts}}{U_{ts}^*} = \frac{\pi h^* v_{\theta cs}^2 \rho_p d_x^2}{9\mu Q}$		(19)
	$\eta_x = 1-\exp\left[-2\left(\frac{C\rho_p d_x^2 v_{in}^2 (n+1)}{18\mu D}\right)^{\frac{0.5}{(n+1)}}\right]$		n is calculated from Equation (64)		(20)
Leith and Licht	$c = \frac{\pi D^2}{ab}\left[2\left(1-\left(\frac{D_e}{D}\right)^2\right)\left(\left(\frac{S}{D}\right)-\left(\frac{\alpha}{D}\right)\right)+\frac{1}{3}(S+t-h)\left(1+\left(\frac{d_c}{D}\right)\right)+\left(\frac{d_c}{D}\right)^2+\left(\frac{h}{D}\right)-\left(\frac{D_e^2}{D}\right)\left(\frac{t}{D}\right)-\left(\frac{S}{D}\right)\right]$				(21)
	$d_c = D-\left(\frac{(D-B)(S+t-h)}{(H-h)}\right)$	(22)	$t = \min\left\{(H-S), 2.3D_e\sqrt[3]{\left(\frac{D^2}{ab}\right)}\right\}$		(23)
Muschelknautz	$\eta = \sum_{i=1}^{N}\eta_i \times \Delta MF_i$	(24)	$C_{0L} = \frac{f D_m \mu}{2\left(1-\frac{D_e}{D}\right)\rho_d d_{med}^2 v_{\theta m}}$		(25)
	$D_m = \sqrt{DD_e}, f' = 0.005\left(13\sqrt{C_0}\right), v_{\theta m}$	(26)	$\eta_x = \frac{1}{1+\left(\frac{d_{50}}{d_x}\right)^m}$		(27)

$$d_{50} = d_{fact}\sqrt{\frac{18\mu(0.9Q)}{2\pi(\rho_p - \rho_g)}v_{\theta CS}(H-S)} \quad (28)$$

Dietz

$$\eta_x = 1-\left(K_0 - \sqrt{K_1^2 + K_2}\right)\exp\left(\frac{-\pi D U_{pw}\left(S-\frac{\alpha}{2}\right)}{Q}\right) \quad (29)$$

$$\begin{cases} K_0 = \dfrac{D_e U_{pw} + D U_{pw} + D_e W_{r0}}{2 D_e U_{pe}} \\ K_1 = \dfrac{D_e U_{pw} + D U_{pw} + D_e W_{r0}}{2 D_e U_{pe}} \\ K_1 = \dfrac{D_e U_{pw}}{D_e U_{pe}} \end{cases} \quad (30)$$

$$U_{pw} = \frac{\rho_p d_x^2 v_{\theta m}^2}{9\mu D}, U_{pv} = \frac{\rho_d d_x^2 v_{\theta e}^2}{9\mu D_e}, \quad (31)$$

$$W_{r0} = \frac{Q}{\pi D_e t}$$

$$v_\theta(r) = v_{\theta w}\left(\frac{D}{2r}\right)^m, (0.5\langle m\langle 1.0) \quad (32)$$

$$t = \min\left\{H-S, 7.3\frac{D_e}{2}\sqrt[3]{\left(\frac{D^2}{4ab}\right)}\right\} \quad (33)$$

Dirgo and Leith

$$\eta_x = \frac{1}{1+\left(\frac{d_{50}}{d_x}\right)^{6.4}} \quad (34)$$

Mothes amd Loffer

$$\eta_x = 1 - \frac{C_4(S)}{C_{0x}} \quad (35)$$

$$C_4(S) = K_1\left(\frac{m_1 - A}{B}\right)b \quad (36)$$

$$K_1 = C_{0x}\exp\left(-\frac{2\pi R_{eq} U_{teq}'\left(S-\frac{\alpha}{2}\right)}{Q}\right) \quad (37)$$

$$m_1 = \left(\frac{A+D}{2}\right) + \sqrt{\left(\frac{A+D}{2}\right)^2 - AD + BC} \quad (38)$$

$$U_{t(r)}' = \frac{d_x^2 \rho_p v_\theta^2}{18\mu r} \quad (39)$$

At $r = R_{eq}, U_{t(r)}' = U_{tR_{eq}}'$

At $r = R_e, U_{t(r)}' = U_{tR_e}'$ (40)

$$R_{eq} = \sqrt{\frac{V_{Cyclone}}{\pi H}} \quad (41)$$

$$v_{rCS} = \frac{Q}{\pi D_e (H-S} \quad (42)$$

When $U_{tR_e}' \rangle u_{rCS}$ (43)

$$A = \frac{2\pi R_{eq} U_{tR_{eq}}'(H-S)}{Q} + \frac{2\pi R_e D(H-S)}{Q(R_{eq}-R_e)} - 1$$

$$B = \frac{2\pi R_e D(H-S)}{Q(R_{eq}-R_e)} - \frac{2\pi R_e\left(U_{rR_{eq}}' - v_{rCS}\right)(H-S)}{Q} \quad (44)$$

$$C = \frac{2\pi R_e D(H-S)}{Q(R_{eq}-R_e)}$$

$$D = B - 1$$

When $U'_{tR_e} \langle u_{rCS}$ (45)

$$A = \frac{2\pi R_{eq} U'_{tR_{eq}} (H-S)}{Q} + \frac{2\pi R_e D (H-S)}{Q(R_{eq}-R_e)} - \frac{2\pi R_e \left(U'_{tR_{eq}} - v_{rCS}\right)(H-S)}{Q} - 1$$

$$B = \frac{2\pi R_e D (H-S)}{Q(R_{eq}-R_e)}$$

$$C = \frac{2\pi R_e D (H-S)}{Q(R_{eq}-R_e)} - \frac{2\pi R_e \left(U_{tR_{eq}} - v_{rCS}\right)(H-S)}{Q}$$

$$D = B - 1$$

$$\eta = \frac{\int_0^\infty m_{in}\eta dd_x}{\int_0^\infty m_{in} dd_x} \quad (46)$$

Lozia

$$d_{50} = \sqrt{\frac{9\mu Q}{\pi \rho_p v_t^2 h^*}}$$ Modified Barth method for V_t and h^*; (47)

$$v_t = 6.1 v_i \left(\frac{ab}{D^2}\right)^{0.61} \left(\frac{D_e}{D}\right)^{-0.74} \left(\frac{H}{D}\right)^{-0.33} \quad (48)$$

$$h^* = \begin{cases} H-S \\ (H-S) - \dfrac{(H-h)}{\left(\left(\frac{D}{B}\right)-1\right)}\left(\left(\frac{d_c}{B}\right)-1\right), \end{cases} \quad \text{if } \begin{cases} d_c \prec B \\ d_c \succ B \end{cases} \quad (49)$$

$$d_c = 0.47 D \left(\frac{ab}{D^2}\right)^{-0.26} \left(\frac{D_e}{D}\right)^{1.4} \quad (50)$$

$$\eta_x = \frac{1}{1+\left(\frac{d_{50}}{d_x}\right)^{-3.2}} \quad (51)$$

Li and Wang

$$\eta_x = 1 - \exp(-\lambda\theta_1) \quad (52)$$

$$\theta_1 = \frac{2\pi(S+t)}{\alpha} \quad (53)$$

$$t \begin{cases} 2.3 D_e \sqrt[3]{\left(\frac{D^2}{ab}\right)} \\ (H-S) \end{cases} \text{ If } \begin{cases} t \prec H-S \\ t \succ H-S \end{cases} \quad (54)$$

$$\lambda = \frac{(1-\alpha) K w_p}{\left(\frac{D_r D^n}{2}\right)} \text{ When } w_p(r) \text{ at } \frac{D}{2} \quad (55)$$

$$D_r = 0.052\left(\frac{D-D_e}{2}\right) v_{in} \sqrt{\frac{f}{8}} \quad f = 0.02 \quad (56)$$

$$K = \frac{(1-n)\left(\rho_p - \rho_g\right) d_x Q}{18\mu b\left(\frac{D^{n-1}}{2} - \frac{D_e^{n-1}}{2}\right)} \quad (57)$$

$$w_p(r) = \frac{d_x^2\left(\rho_g - \rho_p\right) v_\theta(r)^2}{18\mu r} \quad (58)$$

$$v_\theta(r) = \frac{(1-n)Q}{b\left(\frac{D^{n-1}}{2} - \frac{D_e^{n-1}}{2}\right) r^n} \quad (59)$$

2.1. Lapple model

Lapple's model provides equations for calculating the collection efficiency of gas cyclones (Eq. (11), Eq. (12)), relating it to the cut-size diameter. This model relies on a force balance theory, assuming that solid particles entering the gas separator are uniformly distributed across the inlet opening and that all particles initially located within half of the inlet width are captured. This process yields a gas cyclone collection efficiency of 50% [53]. Subsequently, Paola and Theodore developed a graphical representation of Lapple's model [52]. A comparison with experimental results from Leith and Dirgo, who investigated grade efficiencies in a Stairmand high-efficiency gas cyclone (305mm diameter) at velocities ranging from 5 to 25 m/s and a solid loading rate of 0.05 g/m^3 [54], revealed that Lapple's theory underestimated collection efficiencies for coarse solid particles and overestimated them for smaller solid particles, resulting in a flatter collection efficiency curve. Lapple introduced a parameter called the revolution number to reconcile the experimental cut-size diameter with theoretical predictions [53]. The cut-size diameter value was determined to be 5 microns by Lapple [53]. However, Leith and Dirgo's experiments [54] found that this parameter ranged from 10 to 25 with increasing inlet velocity, thereby limiting the theory's applicability to specific conditions. Gimbun et al. [55] have numerically generated several grade efficiency curves based on Lapple's model under varying initial conditions, such as high temperature and high pressure.

2.2. Barth Model

Barth proposed an alternative collection efficiency model, also linking efficiency to the cut-size diameter. This model relies on balancing the drag force and centrifugal force to determine the terminal settling velocity ratio. Equations (13)-(19) outline the governing equations of this theoretical framework. A comparison of its empirical predictions with data from Xiang et al. [56] and Griffiths and Boysan [47] suggests that the Barth model provides reasonable accuracy.

2.3. Lieth and Litch Model

In 1991, Leith and Licht developed a pioneering theory to predict the grade efficiency curve, incorporating the average residence time and flow behavior within a gas cyclone [57]. Their approach correlated collection efficiency with particle residence time, enabling a deterministic evaluation of particle trajectories. Equations (20)-(23) represent this theoretical framework. However, the theory relies on certain assumptions, such as uniform mixing of gas and particles injected at each cross-section, leading to progressive cleaning near the exit. This approach neglects back-mixing between the two vorticities within the gas cyclone. Several researchers have demonstrated the existence of a concentration gradient in the radial direction of gas separators [58–60]. This concentration gradient contradicts the assumption of complete mixing, and the use of deterministic particle trajectories is also inconsistent with the assumption of fully mixed particles. Dietz argued that using average residence time in calculations would effectively reduce the predicted grade efficiencies, making the theory unable to accurately predict gas cyclone collection efficiency [51]. Conversely, Staimand's experimental determination of the grade efficiency curve aligns well with Leith and Licht's theory, as noted by Lieth and Mehta [57]. In contrast to this agreement, other researchers have shown the theory to be inadequate for evaluating experimental collection efficiency curves and particle size diameters [61–63]. Clift et al. [64] improved the Leith and Licht model equations to account for particle removal on the walls and to consider the effects of varying conditions on the S-shaped efficiency curve, which has been reported by numerous researchers. Although Clift's equation applied the internal volume of a gas cyclone from Danckwerts without accounting for inlet and outlet configurations, it enabled estimation of the residence time [61]. Further, Clift et al.'s [64] re-derived correlations showed good agreement with experimental results from Dirgo and Leith [54], but poor agreement with Xiang et al. [56].

2.4. Muschelknautz Model

Muschelknautz et al. developed a theory that refined Barth's model by incorporating the effects of wall roughness, secondary flow, particle loading, and changes in particle size distribution within the gas cyclone on its overall performance [65,66]. This refined model is currently considered a practical approach for modeling gas cyclones [67]. The model is based on the concept of critical loading, which describes the number of solid particles transported in a turbulent suspension. The related equations are presented in Eqs. (24)-(28). However, findings from experimental studies conducted by Hofmann et al. suggest that this approach may not accurately represent critical loading phenomena [68].

2.5. Dietz Model

Dietz [69] proposed a model for cyclone separator collection efficiency, building upon the work of Leith and Licht [57] by incorporating three distinct flow regions (entry, annular, and core), informed by Linden's experimental

observations [70]. A key distinction from previous models was the consideration of particle exchange between the annular and core regions. However, Dietz retained the assumption of uniform radial particle concentration within each region, similar to Leith and Licht [57], and neglected axial back-mixing. Although Dietz's model [69] showed reasonable agreement with Stairmand's experimental data [71], Clift et al. [64] critiqued it for predicting physically unrealistic discontinuities in particle concentration between the annular and core regions. They posited that the model's alignment with experimental data was likely fortuitous rather than a reflection of the model's underlying theory.

2.6. Dirgo Model

Dirgo and Leith empirically adjusted Barth's equation for terminal velocity ratios by increasing it fourfold to achieve better agreement with their experimental observations. This modification resulted in a simplified mathematical expression of Barth's graphical representation, which correlates collection efficiency with the terminal velocity ratio (Eq. (34)) [54].

2.7. Mothes and Loffer Model

Mothes and Löffler [60] critiqued Muschelknautz's [65] concept of critical loading and refined Dietz's [69] model by introducing a new flow region in proximity to the cyclone's dust exit to account for particle re-entrainment. They then incorporated particle agglomeration, calculating impact and sticking probabilities. This approach further integrated turbulent diffusivity in both the annular and core regions. Unlike Dietz's [69] model, this framework removes discontinuities in particle concentration, analyzes particle trajectories, and combines diffusive motion (which affects grade efficiency) with deterministic mean motion (which primarily dictates the cut-size diameter, d50) [51,72]. The intricate theoretical derivations of this model are detailed in Equations (35)-(45). Clift et al. [64] and Gao et al. [73] have demonstrated the model's good agreement with experimental data. A limitation, however, remains: Clift et al. [64] also highlighted that the model's predictive capability is hindered by the challenge of accurately estimating the particle dispersion coefficient, which reflects the effective turbulent diffusivity.

2.8. Iozia and Leith Model

Iozia and Leith [62] modified the Barth model, introducing distinct equations (Eqs. (46)-(50)) to improve its fit with their own cyclone geometry experiments. They reported significant consistency between the modified model and their experimental data. This assessment was corroborated by Xiang et al. [56], who found that Iozia and Leith's adapted model offered a more accurate representation compared to the original Barth theory [74] than did the Leith and Licht [57] variant. Conversely, Griffiths and Boysan [47] noted a sharp divergence between these findings and experimental results reported by Kim and Lee [63].

2.9. Mothes and Loffer

Li and Wang deviated from traditional cyclone flow region separation by concentrating on the influence of finite turbulent particle diffusivity in generating radial concentration gradients. Their model, represented by Eqs. (51)-(58), achieved this by neglecting turbulent particle dispersion within the cyclone's core while still accounting for the particle concentration gradient. Conversely, they posited a zero particle concentration gradient at the walls but incorporated a finite turbulent diffusivity, effectively including particle bounce/re-entrainment and turbulent diffusion at the cyclone wall. Li and Wang asserted that their model provided superior predictive capabilities after validating it against the Dirgo and Leith experimental data [54] and other theoretical models. However, this assessment was subsequently challenged by Kim and Lee [63], who raised concerns about implausibly high tangential velocities, unrealistic wall boundary conditions, and a failure to conserve particle numbers. Numerical analyses by Jolius et al. [55] suggested that Li and Wang's model [75] demonstrated superior predictive accuracy compared to other collection efficiency models [53,62] when evaluated against experimental data from Kim and Lee [63], Dirgo and Leith [54], and Ray et al. [76].

3. Pressure Drop

Dimensional analysis is a useful tool for determining the key variables and structuring both empirical and theoretical formulas related to pressure drop in cyclones. As an example, following the approach of reference [77], we arrive at a relatively comprehensive list of variables.

$$\xi_c = \frac{\Delta P_c}{\frac{1}{2}\rho_g V_{in}^2} = f\left(Geometry, Fr_c, C_{si}, \mathrm{Re}_c, \rho_s \Big/ \rho_g\right) \tag{60}$$

The dimensionless pressure drop, xc (also referred to as the Euler number, Eu), is conventionally defined in terms of the inlet gas velocity, although alternative definitions are viable. As is typical in turbulent flow regimes, the

influence of the Reynolds number is only significant up to a particular threshold and is typically negligible under practical operating conditions. The Froude number (Frc = vi^2/gDc) and solid-to-gas density ratio (ρs/ρg) can be eliminated because their variation is small under typical cyclone designs and operating conditions. Moreover, they have no effect in dilute flow conditions:

1- To generate the new computational model, the total pressure drop inside a gas cyclone was divided into four parts.

2- The pressure drop caused by the expansion of the gas stream as it enters the separator.

3- Pressure drop caused by wall friction within the separator's internal volume.

4- Pressure drop caused by the rotational component of the gas flow.

5- Pressure drop resulting from gas flow through the outlet tube.

The pressure drop caused by the expansion of the gas stream as it enters the separator was calculated as follows:

$$\Delta P_{in} = \xi_{in}\left(\frac{1}{2}\rho_g V_{in}^{\,2}\right) \tag{61}$$

2.1- The pressure drop caused by the expansion of the gas stream as it enters the separator

This pressure drop calculation is based on the idealized condition of uniform flow from the right pipe into the limited space, and the result is given by:

$$\xi_{in} = \left[1 - \frac{ab}{(R_w - r_e)H}\right] \tag{62}$$

2.2- Pressure drop caused by wall friction within the separator's internal volume

The pressure loss caused by friction against the walls inside a separator can be analyzed as if it were in a state of static equilibrium within cyclone separators:

$$\Delta P_{fr}\left[\frac{1}{4}\pi\left(D^2 - d_e^2\right)\right] = c_l\left[\overline{\tau_{\theta ev}}\left(DL\pi\right)\right] \tag{63}$$

The factor cl adjusts for the swirling flow in relation to how evenly the flow is distributed at the wall of the cyclone separator. This adjustment is done according to the Shepherd and Lapple method.

$$c_l = \frac{D\pi}{a} \tag{64}$$

The average shear stress ($\bar{\tau}\theta ev$) of the gas in the outer vortex can be determined using Fanning's equation.

$$\overline{\tau_{\theta ev}} = f\left(\frac{1}{2}\rho_g \overline{v_{\theta ev}}^{\,2}\right) \tag{65}$$

where f = 0.0055

The mean tangential velocity ($\bar{v}\theta w$) of the external vortex can be determined from:

$$\overline{v_{\theta ev}} = \frac{1}{(R_w - r_e)}\int_{r_e}^{R_w} V_\theta dr \tag{66}$$

The result of combining the previous equations is:

$$\Delta P_{fr} = \frac{\left(\pi\frac{D}{a}\right)(\pi DL) f}{\frac{1}{4}\pi\left(D^2 - d_e^2\right)}\left[\frac{\int_{r_e}^{R_w} V_\theta dr}{(R_w - r_e)V_{in}}\right]^2\left(\frac{1}{2}\rho_g V_{in}^2\right) \tag{67}$$

2.3- Pressure drop caused by the rotational component of the gas flow

If axial effects are negligible, the Navier-Stokes equation in cylindrical coordinates can be simplified to show the relationship between pressure and 3D velocity.

$$\frac{dP}{dr} = \frac{\rho_g V_\theta^{\,2}}{r} \tag{68}$$

Zhao [78] proposed the following expression to represent the circumferential flow pattern or velocity profile, incorporating the effect of wall roughness:

$$V_\theta = \frac{V_{\theta w}}{\left(r/R_w\right)\left[1 + P\left(1 - r/R_w\right)\right]} \tag{69}$$

$$V_{\theta w}^{\,*} = V_d \frac{\pi R_w^2}{ab\left[-0.204\left(b/R_w\right) + 0.889\right]} \tag{71}$$

$$V_d = \frac{Q}{\pi R_w^2} \tag{72}$$

$$h^* = \frac{a}{R_w}\left[\frac{2\pi - \arccos\left(b/R_w - 1\right)}{2\pi} - 1\right] + \frac{h}{R_w} \tag{73}$$

$$P = \frac{V_{\theta w}}{V_d}\left(\xi + \frac{\xi}{\sin\varepsilon}\right) \tag{74}$$

$$Q = (ab)V_{in} \tag{75}$$

where $\xi = 0.0065$

Although the expression for V_θ looks complicated, the result agrees very well with the typical velocity profile based on the power-law correlation of Alexander [79].

$$\Delta P_{vf}=\left[\int_{r_e}^{R_w}\frac{2\left(\frac{V_{\theta w}}{V_d}\right)^2\left(\frac{ab}{\pi R_w^2}\right)^2}{r\left(\frac{r}{R_w}\right)^2(1+P-\frac{\Pr}{R_w})^2}dr\right]\left(\frac{1}{2}\rho_g V_{in}^2\right) \quad (76)$$

2.4- Pressure drop resulting from gas flow through the outlet tube

This pressure drop accounts for both local pressure losses and friction-related pressure losses in the outlet pipe.

$$\Delta P_{out}=\Delta P_{ol}+\Delta P_{of} \quad (77)$$

The localized pressure drop was treated as a gas flow contraction loss as the gas moves from the cyclone body to the outlet pipe.

$$\xi_{ol}=\frac{1}{2}\left(\frac{ab}{\pi r_e^2}\right)\left[1-\left(\frac{r_e}{R_w}\right)^2\right]\left(\frac{1}{2}\rho_g V_{in}^2\right) \quad (78)$$

Due to the strong swirling flow, the outlet pipe's pressure drop was calculated similarly to the pressure drop from wall friction inside the separator.

$$\Delta P_{of}\left(\frac{1}{4}\pi d_e^2\right)=c_2'\left[\overline{\tau_{\theta iv}}.\pi d_e\left(S+\Delta S\right)\right] \quad (79)$$

$$c_2'=\frac{\pi d_e}{d_e} \quad (80)$$

$$\overline{\tau_{\theta iv}}=f\left(\frac{1}{2}\rho_g\overline{V_{\theta iv}}^2\right) \quad (81)$$

$\bar{\tau}_{\theta iv}$ represents the average shear stress of the gas in the internal vortex, and $\bar{v}_{\theta iv}$ is the average tangential velocity in the same vortex. We can estimate $\bar{v}_{\theta iv}$ by assuming it's equal to the tangential velocity at a radius of r = r_e.

$$\overline{V_{\theta iv}}=\frac{V_{\theta w}}{\left(r_e/R_w\right)\left(1+P-\Pr_e/R_w\right)} \quad (82)$$

Combining and transforming these equations leads to:

$$\xi_{of}=\frac{\pi^2\left(S+\Delta S\right)f}{\frac{1}{4\pi d_e}}\left[\frac{V_{\theta w}/V_d}{\left(\frac{r_e}{R}\right)\left(1+P-\frac{\Pr_e}{R_w}\right)}\frac{ab}{\pi R_w^2}\right] \quad (83)$$

2.5- Total pressure drop

In summary, the formula for the overall pressure loss is:

$$\Delta P=\Delta P_{in}+\Delta P_{fr}+\Delta P_{vf}+\Delta P_{out} \quad (84)$$

Cyclone pressure drop is often characterized by the pressure drop coefficient (PDC), ξ, which is a measure of gas inlet velocity heads and is solely determined by the cyclone's physical dimensions. Its definition is given by:

$$\xi=\frac{\Delta P}{1/2\,\rho_g V_{in}^2} \quad (85)$$

Existing theoretical models designed to predict pressure drop in cyclones are continuously being refined; however, limitations persist, precluding their universal applicability across all experimental conditions. Several of the more commonly employed models are summarized in Table 2.

Table 2. Theoretical Formulations for Pressure Drop Prediction

Model	Correlation		Remark
Shepherd and Lapple	$\Delta p=\frac{\rho_g v_{in}^2}{2}\left(\frac{16ab}{D_e^2}\right)$	(86)	Tangential inlet; ambient air conditions
Stairmand	$\Delta P=\frac{\rho_g v_e^2}{2}\left[1+2q^2\left(\frac{2(D-b)}{D_e}-1\right)+2\left(\frac{4ab}{\pi D_e^2}\right)^2\right]$	(87)	
	$q=\frac{-\left(\frac{D_e}{2(D-b)}\right)^{0.5}+\left(\frac{D_e}{2(D-b)}+\frac{4A_R G}{ab}\right)^{0.5}}{\left(\frac{2A_R G}{ab}\right)},(G=0.005)$	(88)	
Barth	$\Delta P_{body}=\frac{\rho_g v_e^2}{2}\left[\frac{1}{\left(\frac{v_e}{v_{\theta cs}}-\frac{(H-S)}{0.5D_e}f\right)}-\left(\frac{v_{\theta cs}}{v_e}\right)^2\right]$	(89)	$K=\begin{cases}3.41 for\ vortex\ finder\ with\ rounded\ edge\\ 4.40 for\ vortex\ finder\ with\ sharp\ edge\end{cases}$
	$\Delta P_e=0.5\rho_g v_e^2\left[\left(\frac{v_{\theta cs}}{v_e}\right)^2+K\left(\frac{v_{\theta cs}}{v_e}\right)^{\frac{4}{3}}\right]$	(90)	
	$\Delta P_{tot}=\Delta P_{body}+\Delta P_e$	(91)	
	$f=0.005\left(1+3\sqrt{C_0}\right)$	(92)	

Muschelknazutz	$\Delta P_{body} = \frac{f A_R \rho_g \left(V_{\theta w} V_{\theta CS}\right)^{1.5}}{1.8Q}$	(93)	Tangential and scroll inlets
	$\Delta P_e = 0.5 \rho_g V_e^{\,2} \left[\left(\frac{V_{\theta CS}}{v_e} \right)^2 + K \left(\frac{V_{\theta CS}}{v_e} \right)^{\frac{3}{4}} \right]$	(94)	
	$\Delta P_{acc} = \left(1 + C_0\right) \frac{\rho_g \left(V_2^{\,2} - V_1^{\,2}\right)}{2}$	(95)	Flow field based on Barth0s model
	$\Delta P_{tot} = \Delta P_{body} + \Delta P_e + \Delta P_{acc}$	(96)	
	$f = f + 0.25 \left(\frac{R}{R_e} \right)^{-0.625} \sqrt{\frac{\eta Fr_e \rho_g}{\rho_{Str}}}$	(97)	
Casal and Martinez	$\Delta P = \frac{\rho_g v_{in}^{\,2}}{2} \left[3.33 + 11.3 \left(\frac{ab}{D_e^2} \right) \right]$	(98)	Comparative study of six correlations

3.1. Shepherd and Lapple Model

The empirical pressure drop model developed by Shepherd and Lapple [80], as represented by Eq. (85), is limited in scope due to its exclusive reliance on gas inlet and outlet dimensions. Consequently, it lacks the capacity to analyze the impact of varying geometric configurations or operational parameters. Nevertheless, Leith and Mehta [57] reported that this model yielded accurate correlation coefficients when applied to their experimental dataset.

3.2. Stairmand Model

Stairmand [81] proposed an alternative theoretical framework, commencing with the development of velocity distribution models based on a momentum balance within the cyclone separator. The subsequent estimation of pressure drop considered factors such as entrance and exit losses, alongside static pressure losses within the vortex. Iozia and Leith [62] further refined Stairmand's model through the calculation of correlation coefficients, as expressed in Eqs. (86)-(87). Consistent with this refinement, Leith and Mehta [57] suggested that this approach is conducive to accurate predictions, as it produces correlation values that are highly congruent with those generated by the Shepherd and Lapple model.

3.3. Barth Model

Barth [74], in his investigation of pressure drop within cyclone separators, proposed a model that considered pressure losses within three distinct regions: the inlet, the cyclone body itself, and the vortex finder. While acknowledging the presence of inlet pressure loss, Barth suggested its impact could be considered negligible in practical calculations. The pressure drop within the cyclone body was primarily attributed to a reduction in swirl velocity along a defined friction surface, a relationship expressed mathematically as Equation (88). A key innovation of Barth's model was its explicit consideration of the friction factor's dependence on solid loading, a parameter often overlooked in alternative theoretical frameworks. Furthermore, Barth formulated a semi-empirical relationship (Equation (89)) to quantify pressure drop within the vortex finder. The predictive accuracy of Barth's model has been substantiated by Leith and Mehta [57], who demonstrated its strong performance across a range of correlations.

3.4. Muschelknautz Model

Muschelknautz [82,83] developed a pressure drop prediction methodology (Equations (92)-(96)) that centers on pressure losses occurring within the cyclone body. These losses are primarily attributed to frictional forces at the wall and energy dissipation within the vortex core. In addition to losses within the cyclone body, Muschelknautz acknowledged the role of the vortex finder, identifying particle loading and flow acceleration as contributing factors. Specifically, the impact of mass loading on pressure drop within the vortex finder was assessed using the Barth equation (Equation (88)) as a computational tool within Muschelknautz's overall framework.

3.5. Casal and Martinez Model

Casal and Martinez [84] proposed a simplified empirical model (Equation (97)) for estimating pressure drop in cyclone separators. This model relies primarily on the geometric dimensions of the inlet and outlet sections of the cyclone. A

notable characteristic of this approach is its independence from other physical properties and operating conditions; the predicted pressure drop remains constant regardless of variations in these parameters.

4. Fluid Flow Pattern

Accurate prediction of particle separation efficiency in cyclone separators hinges on a comprehensive understanding of the internal flow field, particularly the distributions of axial, tangential, and radial velocity components. Of these components, tangential velocity is paramount, as it constitutes the primary driving force behind particle separation. While axial and radial velocities contribute to the overall flow dynamics, their influence on separation efficiency is secondary to that of tangential velocity. Consequently, considerable research effort has been dedicated to developing models that predict tangential velocity profiles within cyclones, a selection of which are summarized in Table 3.

Table 3. provides a compilation of theoretical models from the literature, all aimed at predicting flow patterns within cyclone separators.

Models	Equations
Alexander	$v_\theta = v_{\theta CS}\left(\frac{R}{r}\right)^n$ (99) $\quad \frac{V_{\theta w}}{V_{in}} = 2.15\left(\frac{A}{DD_e}\right)^n$ (100)
	$n = 1-(1-0.67D^{0.14})\left(\frac{T}{283}\right)^{0.3}$ (101)
Barth	$V_{\theta CS} = V_x\left(\frac{R_x R_{in}\pi}{ab\alpha + h^* R_{in} f\,\pi}\right)$ (102) $\quad \alpha = 1-0.4\left(\frac{b}{D}\right)^{0.5}, R_{in} = R-\left(\frac{b}{2}\right)$ (103)
	$h^* = \begin{cases} H-S \\ \frac{(H-S)(D-D_e)}{(D-B)} + (h-S) \end{cases}, \begin{cases} D_e \le B \\ D_e \succ B \end{cases}$ (104) $\quad f = 0.02$ (105)
Muschelknautz	$V_{\theta CS} = \frac{V_{\theta w}}{R_e}\frac{R}{\left[1+\frac{fV_{\theta w}A_R\sqrt{\frac{R}{R_e}}}{2Q}\right]}$ (106) $\quad V_{\theta w} = \frac{V_{in}R_{in}}{\alpha R}$ and $\xi = \frac{b}{R}$ (107)
	$\alpha = \frac{1}{\xi}\left(1-\sqrt{1+4\left[\left(\frac{\xi}{2}\right)^2-\frac{\xi}{2}\right]\sqrt{1-\frac{\left(1-\xi^2\right)\left(2\xi-\xi^2\right)}{1+C_0}}}\right)$ (108) $\quad f = 0.005\left(1+3\sqrt{C_0}\right)$ (109)
Meissner and Loffler	$V_\theta(r) = 1+\frac{V_{\theta w}}{\frac{r}{R}\left[<V_z>\left(f_{tid}+\frac{f_{cone}}{Sin\varepsilon}\right)\left(1-\frac{r}{R}\right)\right]}$ (110) $\quad \frac{V_{in}}{V^*_{\theta w}} = -0.204\frac{b}{R}+0.889$ (111)
	(To calculate $V_{\theta CS}$, insert r=Re)
	$V_{\theta w} = \frac{<V_z>}{f_{cyl}H^*_{cyl}}\left[\sqrt{\frac{1}{4}}+f_{cyl}H^*_{cyl}\frac{V^*_{\theta w}}{<V_z>}-\frac{1}{2}\right]$ (112) $\quad H^*_{cyl} = \frac{\alpha}{R}\left[\frac{-\arccos\left(1-\frac{b}{R}\right)}{2\pi}\right]+\frac{H_{cyl}}{R}$ (113)
	$\frac{0.0065 < f_{cyl}}{f_{tid}} / f_{cone} < 0.0075$ (114)

4.1. Alexandra Model

Alexander [85] is credited with pioneering the development of a theoretical model (Equations (98)-(100)) for predicting flow patterns within cyclone separators. His model, based on purely empirical correlations, relates the ratio of tangential velocity at the wall to the mean inlet velocity. This relationship is specifically applicable at high Reynolds numbers. Alexander also proposed a method for characterizing viscosity variation with gas temperature using an exponent. However, the applicability of Alexander's model is limited to cyclone separators with smooth walls and operating under low solid loading conditions [47]. Furthermore, the model's underlying assumption – that swirling velocity at the wall equals the inlet velocity, irrespective of inlet geometry – has been identified as a potential flaw. Patterson and Munz [70] observed that while Alexander's model provides reasonable predictions of tangential velocity at ambient temperatures, its accuracy diminishes at elevated temperatures, and it exhibits a high sensitivity to geometric parameters. Supporting the significance of these parameters, Zhao et al. [73] found good agreement between their experimental results and those predicted by Alexander's model, while also emphasizing the complex nature of the vortex exponent n. They noted that the value of n is influenced by a combination of factors including Reynolds number, cyclone geometry, and wall roughness.

4.2. Barth Model

Barth's empirical model [86] posits the existence of a hypothetical cylindrical core, extending downward from the vortex finder along the central axis of the cyclone separator to the bottom. This conceptual core is defined by its height and diameter. A significant contribution of Barth's model lies in its pioneering attempt to incorporate the influence of both wall friction and cyclone geometry on the tangential velocity components within the cyclone. The core equations underpinning this model are detailed in Equations (101)-(104).

4.3. Muschelknautz Model

Muschelknautz expanded upon Barth's model to develop a more sophisticated framework for predicting flow patterns within cyclone separators. This advancement incorporated the effects of both wall friction and mass loading, thereby providing a more realistic representation of the internal flow dynamics. The mathematical formulations underlying this framework are detailed in Equations (105)-(110).

4.4. Meissner an Loffer Model

Meissner and Löffler [70] proposed a method, detailed in Table 3, for predicting the flow field within cyclone separators based on a momentum balance approach (Equations 111-113). This method involves dividing the flow domain into vertical cylindrical elements and equating the momentum influx and efflux with the frictional forces acting at the top and bottom surfaces. The model simplifies the analysis by neglecting wall friction along the cylindrical body. However, the Meissner and Löffler method exhibits several limitations. It is primarily applicable to cyclone separators with slot-type inlets and cylinder-on-cone configurations. Furthermore, its accuracy is compromised under high mass loading conditions, as it does not consider the influence of dust deposition on the wall friction factor. Empirical validation by Patterson and Munz [70] and Zhao et al. [73] suggests that this method tends to overestimate experimental measurements. cylindrical elements and balancing the momentum entering and exiting with the frictional forces at the top and bottom of the cyclone, while neglecting the wall friction of the cylindrical body. However, it is limited to predicting flow patterns in cyclone separators featuring slot-type inlets and cylinder-on-cone designs. Additionally, it is only suitable for low mass loading conditions, as it does not account for the impact of dust deposition on the wall friction factor. Furthermore, this model tends to overestimate the experimental data from Patterson and Munz [70] and Bingtao et al. [73].

5. Results and Discussion

5.1. Collection Efficienc

The divergence between the current study's findings and the predictions of Li and Wang's theory may be attributable to the elevated particle concentrations employed in the experimental setups of Dirgo and Leith [54] and Kim and Lee [63]. While the Lapple method provided satisfactory estimations of collection efficiency for particles within the 2.0 - 10.0 μm range across two tested velocities, it demonstrated a tendency to underestimate efficiency for finer particles. A key parameter in the Lapple model, the number of turns (N), is inherently dependent on specific cyclone design and inlet velocity, introducing a potential source of error; in these calculations, a fixed value of 12 was used. The Mothes and Löffler theory exhibited good agreement with experimental data for particle sizes between 5.0 and 10.0 μm at a velocity of 10 m/s. Across all theoretical models, consistency with experimental results was observed for particles exceeding 10.0 μm. However, at a reduced velocity of 5 m/s, the

theoretical grade efficiencies for fine particles (< 5.0 μm) tended to be underestimated, although alignment improved for particles larger than 5.0 μm. The most pronounced discrepancies were observed for the Mothes and Löffler and Li and Wang theories. A potential contributing factor to the inaccuracies of Barth, Li and Wang, and Mothes and Löffler's theories lies in their treatment of wall friction. While these models account for a constant effect of wall friction, this simplification may not adequately represent the complex relationship between friction and varying particle loading rates within the cyclone. Furthermore, Mothes and Löffler's assumption of constant turbulent diffusivity may not accurately reflect the turbulent flow regime within the cyclone separator. The Leith and Licht model consistently overestimated grade efficiencies, producing a flatter curve in contrast to the typical 'S-shaped' curve (Fig. 5). This behavior is likely a consequence of the model's assumption of uniform mixing of gas and particles at each axial cross-section, leading to distinct and potentially unrealistic grade efficiency predictions. This pattern aligns with observations reported by Griffiths and Dirgo and Leith [54], Clift et al. [64], Boysan [47], and Kuo and Tsai [87], suggesting a systematic limitation of the Leith and Licht approach. Muschelknautz's theory stands out due to its consideration of particle loading effects. However, analysis of the grade efficiency curves generated by this theory reveals inconsistencies between the dfact parameter (as defined by Muschelknautz) and the experimental data obtained in this study. The original theory posits a dfact range of 0.9 to 1.4, whereas calculations based on experimental results yielded a significantly broader range of 0.18 to 3.2. Similarly, the theory prescribes a slope (m) between 2.0 and 7.0, while the present study determined a range of 0.18 to 1.8. Therefore, a critical re-evaluation of the dfact parameter and its underlying assumptions is warranted to more accurately assess the applicability of Muschelknautz's theory to the experimental conditions investigated here.

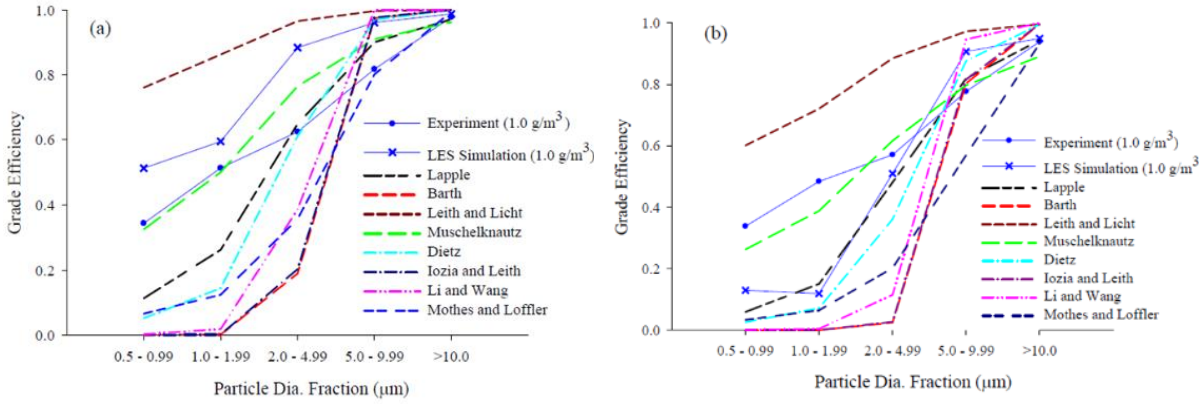

Fig. 5. Presents a comparative analysis of theoretical grade efficiency curves with experimental data obtained from [57] and numerical simulation results from[88]. This comparison is performed to assess the validity of the theoretical models at two distinct inlet velocities: (a) 10 m/s and (b) 5 m/s.

5.2. Pressure Drop

Pressure drop calculations were performed using the theoretical models developed by Stairmand [71], Barth [74], Shepherd and Lapple [80], Casal and Martinez [84], and Muschelknautz [66,89]. These theoretical values were subsequently compared with both experimentally derived and numerically simulated pressure drop data (Table 4). The models proposed by Stairmand and Barth estimate pressure drop based primarily on pressure losses at the inlet and outlet, coupled with swirling losses within the cyclone body. However, these models do not account for the influence of solid loading, a factor demonstrated to be significant in numerous studies [90–93]. In practical cyclone applications, relying solely on inlet and outlet pressure losses may be insufficient due to the considerable pressure drop occurring within the dust collection section.

This section is critical in influencing the overall pressure drop, as processes such as sudden extraction, swirling effects, and high particle concentration zones contribute substantially to energy dissipation. Consequently, the observed overestimation of theoretical pressure drops predicted by the Stairmand and Barth models likely underscores the significance of these factors. The purely empirical models of Shepherd and Lapple and Casal and Martinez offer an analysis predicated on experimental data, but they potentially neglect the relevance of operational conditions by focusing primarily on the cyclone's inlet and vortex finder outlet. In the present study, the Casal and Martinez model overestimated pressure drops, while the Shepherd and Lapple

model exhibited relatively more accurate predictions. While the Shepherd and Lapple model produced the closest agreement with experimental data among the tested theories, the underlying reasons for this accuracy remain unclear. A possible explanation relates to the specific pressure drop sampling points utilized in the experiment. As highlighted in the study by Bogodage and Leung [48], pressure drops were measured between the inlet and an outlet location not positioned at the vortex finder, complicating the assessment of the Shepherd and Lapple model's accuracy in that context. Nevertheless, some general inferences can be made, acknowledging the potential influence of pressure drops arising from sudden contractions in cyclone separators and expansions at the inlet and outlet on swirling losses within the cyclone body. Despite incorporating wall friction losses associated with solid loading and vortex core losses via calculated pressure drops, Muschelknautz's mechanistic theory also overestimated experimental pressure drop values. Indeed, this model yielded the most substantial overestimation of pressure drops relative to all other tested theories.

Table 4. Pressure drop data at inlet velocities of 1 and 2 m/s, illustrating the agreement between experimental measurements, numerical simulations, and theoretical predictions based on [mention models used, if relevant

Method	Pressure drop[Pa]	
	At 5 m/s	At 10 m/s
Experimental (at solid loading rate of 1 g/m^3)	37.30	157.05
Numerical (LES method) (at solid loading rate of 1 g/m^3)	43.8	198.74
Shepherd and Lapple	38.75	155
Stairmand	60.31	241.25
Bath	70.66	282.3
Casal and Martinez	54.36	217.47
Muschelknautz (at solid loading rate of 1 g/m^3)	136.91	336.25

5.3. Flow Patterns in gas cyclone

As various cyclone designs [94] illustrated by earlier flow pattern models, the design from ter Linden [95] demonstrates that each axial design is different but very similar, as shown in Figure 6. The important forces are the various axial forces, where an overall Rankine design is what should be achieved. The different components have allowed a more centralized design in both axial and various changes.

The Rankine model best uses the key velocity exponent n. That value is between 0.5 and 0.9 and can be influenced by a great number of factors, such as the design, with cyclone diameter having a significant effect, but they are often very linked and connected. In particular are designs where the Reynolds Number is relevant, where if a smaller diameter is used, there must be increased loading and temperature, which would further decrease the value [57,96]. The designs from (0.96-1) show the high correlation is found to be similar between most of the velocity numbers. This relation also finds that different diameters and such often can show where the location between different quasars may exist in Fig. 7, compared with experimental data.

This study investigates the accuracy of several established theoretical models in predicting tangential velocity profiles within a cyclone separator, a crucial aspect of swirling flow behavior. The models developed by Alexander [79], Meissner & Löffler [97], Barth [74], and Muschelknautz [89] (summarized in Table 3) were employed to calculate tangential velocity, and their predictions were compared with computational fluid dynamics (CFD) results for an inlet velocity of 10 m/s (Fig. 8). Due to the absence of experimental data for validation, the analysis focuses solely on comparing the theoretical predictions with the numerical simulations. The results reveal that the empirical models of Alexander and Meissner & Löffler, while capable of capturing the tangential velocity field in the outer vortex region, tend to overestimate the velocity magnitude. The incorporation of a wall friction factor in Meissner & Löffler's model did not demonstrably improve the accuracy of their predictions.

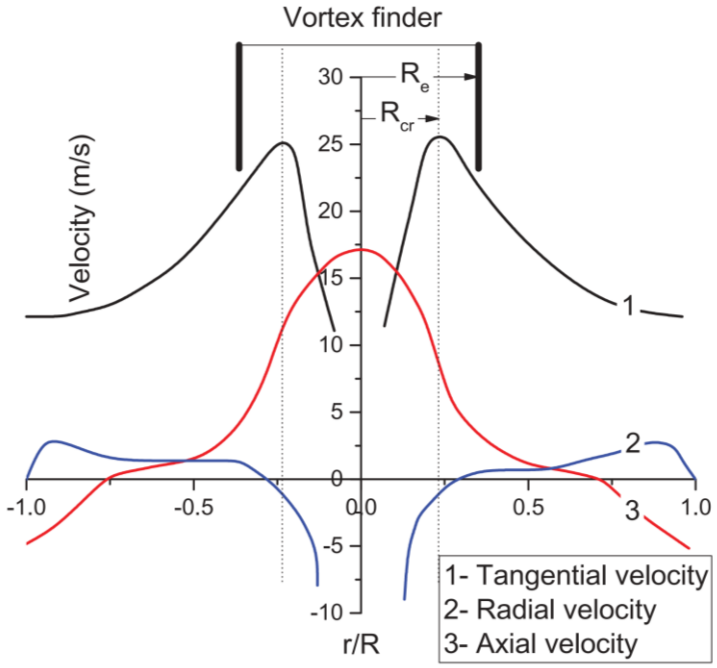

Fig. 6. Flow pattern in a conventional gas cyclone [95]

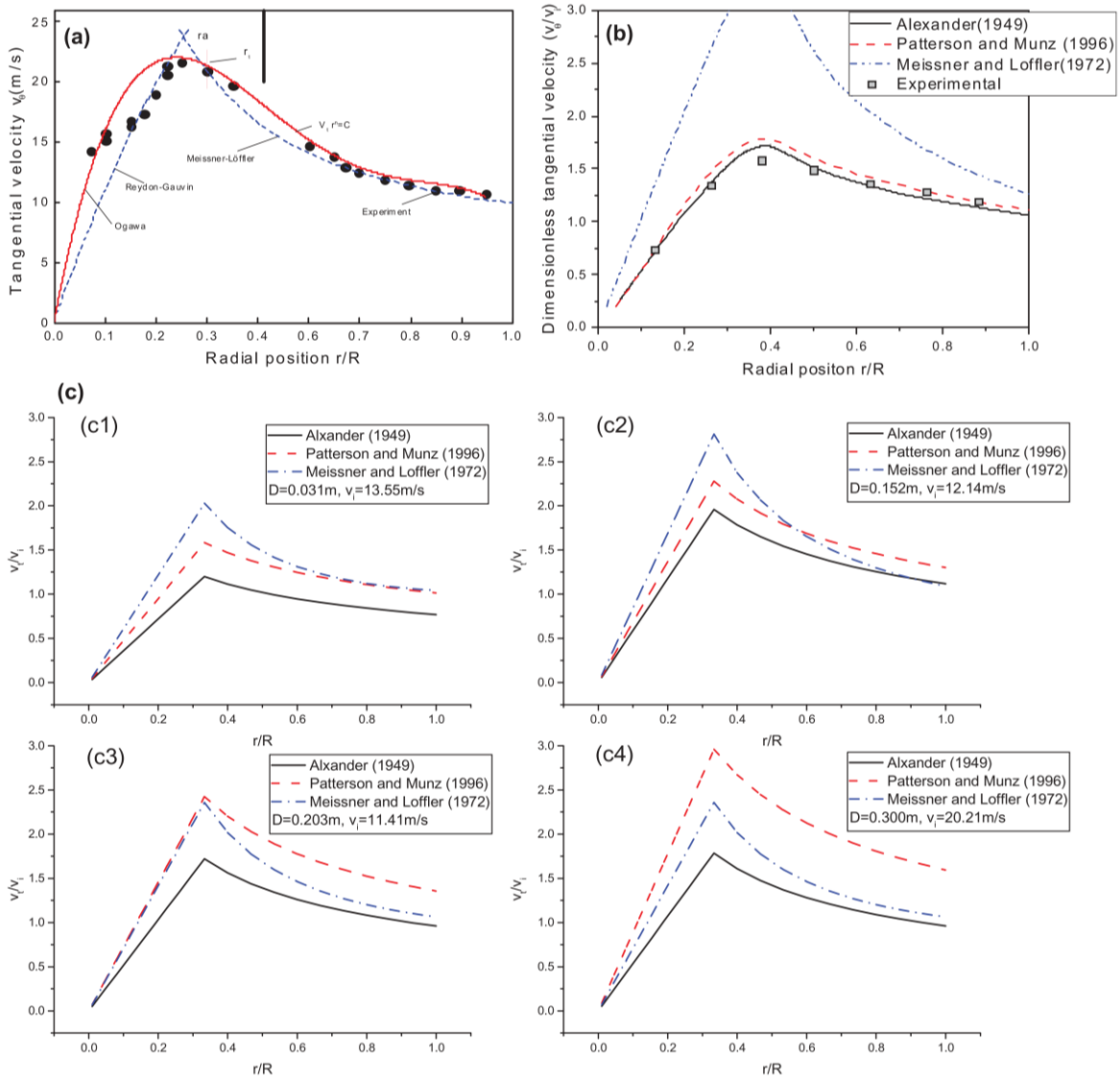

Fig. 7. Experimental model compare with each other under different conditions [73]

Similarly, the theoretical models of Barth and Muschelknautz, which incorporate both the tangential velocity at the control surface and the wall friction factor, also overpredicted the tangential velocity when compared to the CFD results. A key limitation of these theoretical models is their inability to predict the actual velocity fields with the same fidelity as those employed for assessing performance parameters. Furthermore, the Large Eddy Simulation (LES) employed in this study utilized a one-way coupling approach, neglecting the influence of the particle phase on the fluid phase. As demonstrated in previous numerical studies by Derksen et al. [98], Qian et al. [99], and Xue et al. [59], the presence of solid particles leads to a reduction in tangential velocity. Consequently, the actual tangential velocities within the cyclone separator are expected to be lower than the numerical results obtained in this study. This discrepancy suggests that the tested theoretical models fail to accurately represent the real-world conditions where particle-fluid interaction significantly impacts the tangential velocity field. Therefore, the discrepancy between the theoretical models and numerical results might be further amplified in a real cyclone separator with a two-way coupling between the particle and fluid phases.

5.4. Solids loading impacts

At low solid-to-gas mass loading ratios (e.g., 0.01 kgs/kgg), solid particles are observed to aggregate into discrete, thin strands along the interior walls of the cyclone, exhibiting a downward spiral trajectory. Conversely, under high mass loading conditions (e.g., 10 kgs/kgg), a substantial fraction of (or the entirety of) the wall surface is enshrouded by a contiguous layer of solid particles (identified as a "dense strand" in [100]), which is then directly conveyed into the solids discharge [89]. Existing experimental work indicates that increasing the inlet solids mass loading ratio typically enhances both overall and grade separation efficiencies in cyclones [46,68,89].

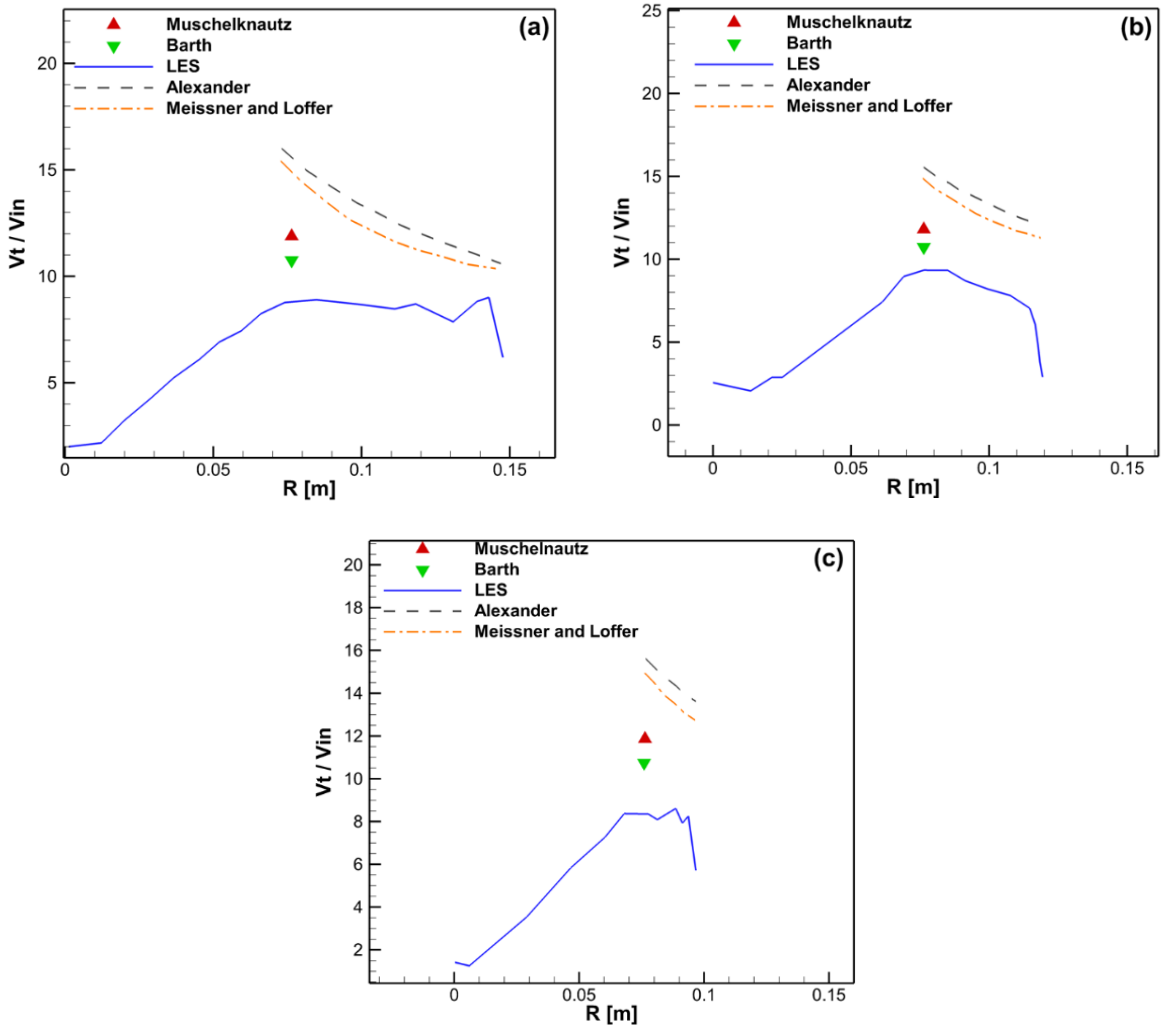

Fig. 8. Theoretical tangential velocities compared with numerical tangential velocities (a) 0.075 m; (b) 0.2 m and (c) 0.3 m downward to the vortex finder inlet.

Hoffmann and Stein [46] demonstrated a marked improvement in grade efficiency for most particle sizes with an increase in mass loading from 3.7×10^{-3} to 2.6×10^{-2} kgs/kgg. However, they also highlighted the interplay between mass loading, inlet gas velocity (swirl strength), and separation efficiency [101]. As shown in Figure 2, the data from [46] suggests that the benefits of increasing cyclone Reynolds number on separation efficiency are most evident at lower mass loadings (below 0.01 kgs/kgg), given a constant kinematic response time of 0.1 milliseconds. The high separation efficiencies reported by Fassani and Goldstein [91] are likely due to the higher kinematic response time of their particles compared to other studies in Figure 9, while the influence of this parameter is inconclusive across the other studies.

While experimental work consistently demonstrates that solids loading influences separation efficiency, the precise mechanism remains debated [46]. Competing theories include the "critical mass loading ratio" (ΦG) of Muschelknautz and Brunner [65,89], where excess particles above a threshold are ideally separated, a theory countered by data from [103], and the agglomeration hypothesis of Mothes and Löffler [104], which attributes the improvements to larger particles that are more easily separated. Hoffmann and Stein [46] propose a more nuanced explanation in which overall improvement is a combined effect of agglomeration for fine particles and reduced drag forces because of concentration. For very fine particles, the agglomeration is particularly dominant, especially with humid carrier gas. They also posit that increased particle concentration reduces drag force, further enhancing separation. Research by Baskakov et al. [105] and Muschelknautz and Brunner [89] indicates that pressure drop in cyclones initially decreases with increasing solids loading before rising again. This trend, also seen in other studies [106–108], is attributed to two competing effects. At low loadings, the reduction in swirl intensity leads to a more pronounced decrease in the pressure loss associated with the vortex finder, thus an overall reduction of pressure drop. When the mass loading is high enough, there is reduced pressure loss in the vortex finder, but an increase in frictional pressure loss at the wall. Therefore, the result is that pressure increases after a minimum value is hit. Figure 10 summarizes experimental data on pressure drop versus solids loading in pilot-scale cyclones, drawn from the literature. While some studies [89,105] report a minimum pressure drop at a specific solids loading ratio, this finding is not universal. A number of studies [92,102] only observe a reduction in pressure drop with increasing mass loading; however, these investigations are limited to smaller mass loadings (less than 0.5 kgs/kgg). Furthermore, other reports indicate that the pressure drop can also increase [109] or remain constant [91] as the inlet solids loading increases, creating a complete disagreement across different studies, designs, and operating procedures.

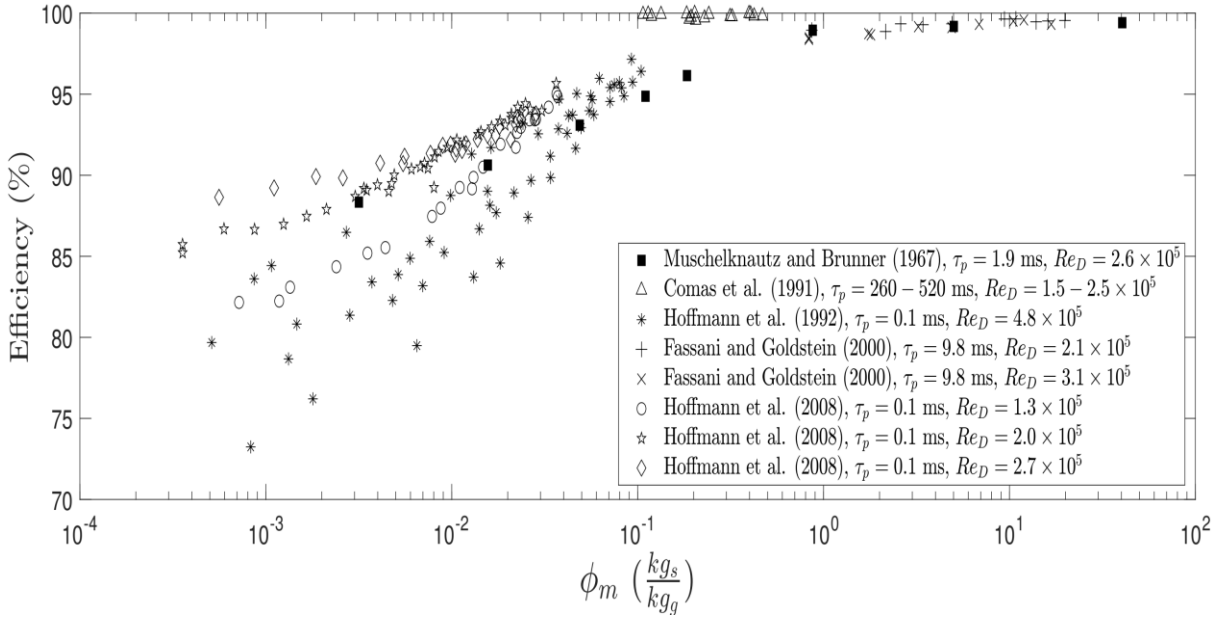

Fig. 9. Shows experimental data gathered from various literature sources [46,102], plotting overall cyclone separation efficiency as a function of the solids mass loading ratio at the cyclone inlet. The Reynolds number, calculated using the inlet velocity and cyclone body diameter, is used to characterize the flow conditions.

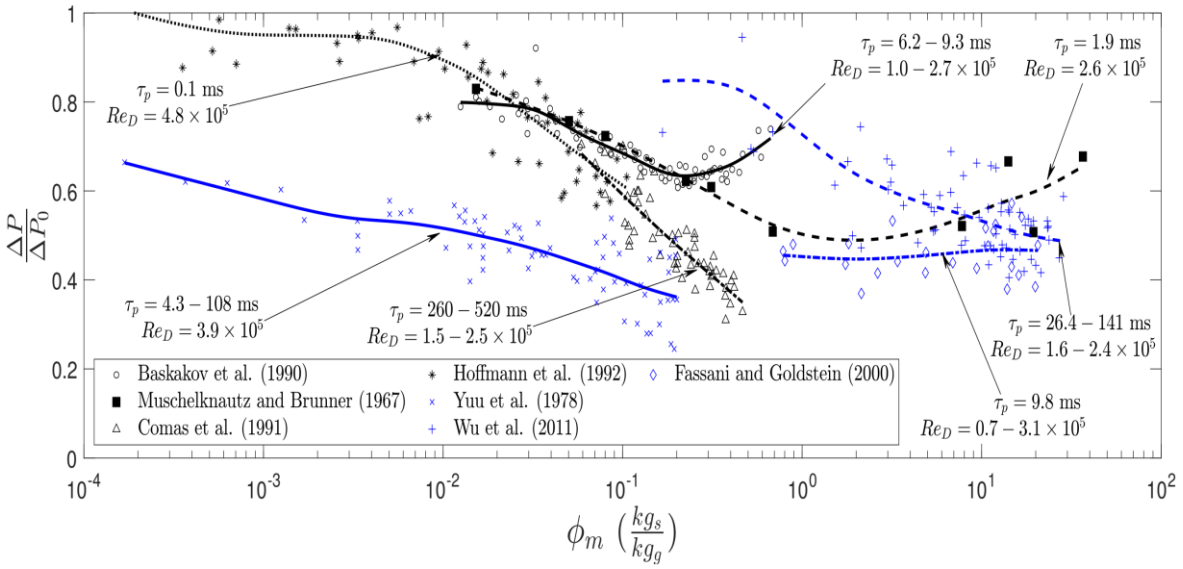

Fig. 10. displays experimental measurements of pressure drop (normalized to a particle-free cyclone,ΔP_0) versus mass loading in pilot-scale cyclones, gathered from various studies [105,110,111] . The data are fitted with numerical curves to highlight the trends. All Reynolds numbers reported use the inlet velocity and cyclone diameter.

5.5. Impact of Gas Temperature

High-temperature cyclones are important for industrial separation in processes such as temperature treating: drying, heating, flue gas cleaning. These units can see solids-gas concentrations from 10-100 kgs/kgg [112]. Therefore, cyclone performance is affected by its temperature and its effect on efficiency, pressure drop, and heat transfer. In general, as gas temperature increases, the gas experiences a decrease in density and an increase in viscosity. At a fixed volumetric gas-flow rate to the cyclone, this change in fluid properties has as direct consequences the reduction of Reynolds Number and thus swirl intensity in the cyclone at elevated operating temperatures, finally resulting in a drop in cyclone pressure drops, as confirmed by many experimental [113,114] and CFD studies [115]. In addition to the previously mentioned effect of temperature on swirl and resulting force, there are a number of studies with strong evidence that temperature leads to both a drag/hindering force through changes in viscosity, but also a less significant change in the particle buoyancy. These combined results are often shown to occur at lower values of Reynolds number, where there is both a reduced centrifugal force from swirling coupled with increased drag in the fluid. Experimental studies have generally found that heat transfer to the particles in gas-solid cyclones is best when increasing both the solid loading and with lower values of Reynolds number, while being inversely influenced by the particles [116]. Higher Reynolds numbers may occur due to the fact that there is a higher degree of stronger coupling, which may prevent gases from bypassing directly into the vortex finder. This results in higher overall temperatures near the bottom and increased heat transfer rates. As noted before, heat transfer at particle loadings will result in some diminishing returns [116,117], where gains are no longer achievable even at those higher loadings as the rate has reached an apex where no gain can occur. Higher gas velocities with particles that are smaller can also lead to a higher degree of overall gas-solid effects [116,117], which is believed to result from an increased amount of temperature available, or surface area where contact can occur. Temperature will lead to erosion as a direct result of both collision or any chemical effects with aggressive species in high refractory. As the wear continues, the roughness will lead to more problems through high particle and collision with the cyclone walls before the change in the movement [118]. It is important to have frequent hardware maintenance for the cyclone, including plate wear, replacement of any part damaged, and a flat disk with vortex. If there is lack of attention, build-ups can happen.

5.6. Natural Vortex Length (NVL)

In the context of gas-particle cyclonic separation, the natural vortex length (NVL) emerges as a critical process parameter alongside three-dimensional velocity fields. The NVL, defined as the axial distance from the vortex finder entrance (or the bottom of the cyclone) to the point where the vortex terminates, directly impacts the residence time and effective separation height available for gas-particle separation. The NVL exhibits complex behavior, as it is not solely determined by the cyclone's physical geometry. Rather, it is significantly

influenced by a combination of factors including the gas Reynolds number, cyclone dimensions (such as inlet area, diameter, and vortex finder length), particle outlet design, wall roughness, and particle loading. Furthermore, the location of the vortex termination point is characterized by inherent instability and randomness, adding complexity to its prediction and control.

Table 5. Different natural vortex length(NVL) modeling

Investigator	Natural vortex Length (NVL)	Range of Lv/D	MAE	MSE
Alexander(1949)[119]	$\frac{L_v}{D}=2.3(D_e/D)\left[D^2/(ab)\right]^{1/3}$	1.24–2.48	1.9579	4.3831
Bryant et al. (1983)[120]	$\frac{L_v}{D}=2.26\left[D_e{}^2/(ab)\right]^{-1/2}$	1.43–2.86	1.7595	4.1130
Mothes & Löffler (1988)[121]	$\frac{L_v}{D}=\left[H-(H-s)/10\right]/D$	2.70–3.15	0.9120	1.1825
Ji et al. (1991)[122] Hoffmann et al. (2001)[123]	$\frac{L_v}{D}=2.4(D_e/D)^{-2.25}\left[D^2/(ab)\right]^{-0.361}$	4.97–23.65	8.9008	145.9467
Qian and Zhang (2005)[124]	$\frac{L_v}{D}=f(D_e/D,a/D,b/D,(h-s)/D,\ln(\mathrm{Re}))^a$	5.01–5.77	1.6539	3.0699
MacLean et al. (1978)[125] Hoffmann et al. (1995)[123]s	$\frac{L_v}{D}=-1.09(\pi D_e^2)/(4ab)+4.49^b$	2.35–3.95	0.9619	1.4925
Li et al. (2016)[126]	$\frac{L_v}{D}=k[D^2/(ab)][1-(D_e/D)^2](k=1.02)$	7.65–9.56	4.8433	24.7882

6. Conclusions

This study critically examines the practical applicability of various theoretical models for predicting cyclone performance and internal flow characteristics, comparing their predictions against both experimental and numerical data. The analysis reveals several significant limitations that hinder their effective use in designing high-efficiency cyclones:

1) Collection Efficiency Models: Existing theoretical models for predicting cyclone collection efficiency, primarily developed under conditions of low solid loading, exhibit significant shortcomings. While Muschelknautz's theory demonstrated some agreement with experimental results, its validation requires further investigation through more extensive experimental data to analyze two specific variables. Other models consistently generated idealized "S-shaped" grade efficiency curves, failing to capture the enhanced fine particle collection observed in real-world scenarios due to particle agglomeration. Furthermore, these models tended to overestimate collection efficiency for coarser particles due to their neglect of particle re-entrainment mechanisms.
2) Pressure Drop Prediction: Accurately predicting pressure drop, a crucial parameter for optimizing the energy efficiency of cyclone designs, remains a significant challenge. Only the purely empirical model proposed by Shepherd and Lapple provided reasonably accurate predictions. However, the overall assessment of accuracy was complicated by inconsistencies in the reported locations of pressure drop measurements across different experimental studies.
3) Flow Pattern Prediction: The prediction of internal flow patterns within cyclones using theoretical models proves challenging due to the complex interplay of particle phase influences and frictional wall effects, which vary spatially within the cyclone. Consequently, the evaluated theories generally failed to accurately predict flow patterns, often resulting in over-predicted velocities.

4) Ambient temperature and solid loading are demonstrated to be key factors that should be considered when using the correct set up. Therefore, as mentioned throughout this research, a detailed review of the literature has shown this. With that, future work can be achieved, with a potential outcome of wear.

5) Natural Vortex Length (NVL) Modeling: Modeling the natural vortex length (NVL) in cyclone separators is characterized by inconsistencies and contradictions, particularly regarding the influence of inlet and outlet areas, leading to significant disparities in predicted outcomes. The accuracy of NVL models is highly dependent on the model's underlying assumptions, specifically whether the inlet velocity or flow rate is used as the primary determinant of NVL. Statistical analysis suggests that Mothes and Löffler's model exhibits superior predictive capabilities for optimized cyclone designs, although it lacks explicit consideration of the gas Reynolds number. Further research, incorporating flow visualization techniques to observe the natural vortex length and investigating the effects of global parameters on NVL, is warranted.

In conclusion, despite decades of theoretical development, no existing cyclone model provides entirely satisfactory predictions across all performance metrics. Key limitations stem from the models' inadequate representation of critical phenomena such as particle agglomeration, particle re-entrainment, and the specific geometry of the dust collection section. Additionally, the models often fail to account for spatial variations in the wall friction coefficient and turbulent diffusivity of particles, particularly under higher solid loading conditions. These factors represent the primary weaknesses of the evaluated theoretical models and highlight areas for future research and model refinement.

Acknowledgments

We acknowledge the use of various figures sourced from other publications throughout this review.

Funding Statement

This research did not receive any specific grant from funding agencies in the public, commercial, or not-for-profit sectors.

Conflicts of Interest

The author declares that there is no conflict of interest regarding the publication of this article.

Authors Contribution Statement

Farzad Parvaz: Conceptualization; writing – original draft; methodology; validation; visualization; writing – review and editing; formal analysis; supervision.

Masoud Dorfeshan: Visualization and restate some sentences

Sadegh Nikbakht Naserabad: Writing – review and editing; visualization; validation

References

[1] Gao, X., Chen, J., Feng, J. and Peng, X., 2013. Numerical and experimental investigations of the effects of the breakup of oil droplets on the performance of oil–gas cyclone separators in oil-injected compressor systems. *International journal of refrigeration*, *36*(7), pp.1894-1904. https://doi.org/10.1016/j.ijrefrig.2013.06.004.

[2] Markt, D.P., Pathak, A. and Raessi, M., 2018. Advanced computational simulations of surface impingement of a train of ethanol drops: A pathway to developing spray-wall interaction submodels. *Computing in Science & Engineering*, *20*(4), pp.56-65. DOI: 10.1109/MCSE.2018.042781326.

[3] Park, D. and Go, J.S., 2020. Design of cyclone separator critical diameter model based on machine learning and cfd. *Processes, 8(11),* p.1521.https://doi.org/10.3390/pr8111521

[4] Parvaz, F., Hosseini, S.H., Elsayed, K. and Ahmadi, G., 2018. Numerical investigation of effects of inner cone on flow field, performance and erosion rate of cyclone separators. *Separation and Purification Technology, 201,* pp. 223-237. https://doi.org/10.1016/j.seppur.2018.03.001.

[5] Dorfeshan. M, Moghaddam. S, Parvaz. F., 2025. The Impression of Roughness on Flow Pattern and Performance of Axial Gas Cyclone Along with Erosion Rate. Journal of Gas Technology, 9(2), pp. 70-87. https://doi.org/20.1001.1/jgt.2025.2057137.1054.

[6] Izadi, M., Makvand, A.M., Assareh, E. and Parvaz, F., 2020. Optimizing the design and performance of solid–liquid separators. *International Journal of Thermofluids, 5,* p.100033. https://doi.org/10.1016/j.ijft.2020.100033.

[7] Vahedi, S.M., Parvaz, F., Kamali, M. and Jafari Jebeli, H., 2018. Numerical investigation of the impact of inlet channel numbers on the

flow pattern, performance, and erosion of gas-particle cyclone. *Iranian Journal of Oil and Gas Science and Technology, 7(4)*, pp.59-78. https://ijogst.put.ac.ir/article_57757.html.

[8] Parvaz, F., 2024. The effect of curves of tangential channel on gas cyclone performance. *Computational Methods in Engineering Sciences, 1(4),* pp.9-18. https://doi.org/10.22034/cmes.2024.2024131.1022.

[9] Parvaz, F., Rafee, R. and Talebi, F., 2018. Effects of the Outlet Pipe Diameter on the Performance of Aerocyclone in Gas Droplet Two-Phase Flow. *Journal of Mechanical Engineering, 48,* pp. 45–53. https://tumechj.tabrizu.ac.ir/article_7816.html.

[10] Vahedi, S.M., Parvaz, F., Rafee, R. and Khandan Bakavoli, M., 2018. Computational fluid dynamics simulation of the flow patterns and performance of conventional and dual-cone gas-particle cyclones. *Journal of Heat and Mass Transfer Research, 5(1),* pp. 27-38. https://doi.org/10.22075/jhmtr.2017.11918.1170.

[11] Parvaz, F., Vahedi, S.M. and Khandan, M., 2018. Numerical investigation of the effects of geometry variation on the flow pattern and performance of Gas-Particle cyclones. *Iranian Journal of Mechanical Engineering Transactions of ISME, 19(4),* pp.101-122.

[12] Dehdarinejad. E, Hossein. S, Parvaz. F, Dehdarinejad. M, Ahmadi. G, Olazar, M., 2026. Comprehensive study on the role of wall roughness in square cyclone performance : Flow field , erosion rate , and separation efficiency. *Chemical Engineering Science*, 321, Part B, p.122860. https://doi.org/10.1016/j.ces.2025.122860

[13] Parvaz, F., Hosseini, S.H., Bastan, A.R., Foroozesh, J., Babaoğlu, N.U., Elsayed, K. and Ahmadi, G., 2023. Influence of gas exhaust geometry on flow pattern, performance, and erosion rate of a gas cyclone. *Korean Journal of Chemical Engineering, 40(7),* pp. 1587-1597. https://doi.org/10.1007/s11814-023-1430-2.

[14] Elsayed, K., Parvaz, F., Hosseini, S.H. and Ahmadi, G., 2020. Influence of the dipleg and dustbin dimensions on performance of gas cyclones: An optimization study. *Separation and Purification Technology, 239,* p.116553. https://doi.org/10.1016/j.seppur.2020.116553.

[15] Parvaz, F., Hosseini, S.H., Elsayed, K. and Ahmadi, G., 2020. Influence of the dipleg shape on the performance of gas cyclones. *Separation and Purification Technology, 233,* p.116000. https://doi.org/10.1016/j.seppur.2019.116000.

[16] Vahedi, S.M., Parvaz, F., Khandan, B.M. and Kamali, M., 2020. Effect of Surface Roughness on Vortex Length and Efficiency of Gas-oil Cyclones through CFD Modelling. *Iranian Journal of Oil and Gas Science and Technology, 9,* pp. 68–84. https://doi.org/10.22050/ijogst.2018.102377.1417.

[17] Dehdarinejad, E., Bayareh, M., Parvaz, F., Hosseini, S.H. and Ahmadi, G., 2023. Performance analysis of a gas cyclone with a converging-diverging vortex finder. *Chemical Engineering Research and Design, 193*, pp.587-599. https://doi.org/10.1016/j.cherd.2023.04.012.

[18] Dehdarinejad, E., Parvaz, F., Hosseini, S.H., Ahmadi, G. and Elsayed, K., 2023. Performance analysis of a gas cyclone with a dustbin inverted hybrid solid cone. *Aerosol Science and Technology, 57(9),* pp.911-924. https://doi.org/10.1080/02786826.2023.2217873.

[19] Foroozesh, J., Parvaz, F., Hosseini, S.H., Ahmadi, G., Elsayed, K. and Babaoğlu, N.U., 2021. Computational fluid dynamics study of the impact of surface roughness on cyclone performance and erosion. *Powder Technology, 389,* pp.339-354. https://doi.org/10.1016/j.powtec.2021.05.041.

[20] Babaoğlu, N.U., Parvaz, F., Foroozesh, J., Hosseini, S.H., Ahmadi, G. and Elsayed, K., 2023. Geometry optimization of axial cyclone for high performance and low acoustic noise. *Powder Technology, 427,* p.118738. https://doi.org/10.1016/j.powtec.2023.118738.

[21] Babaoğlu, N.U., Parvaz, F., Hosseini, S.H., Elsayed, K. and Ahmadi, G., 2021. Influence of the inlet cross-sectional shape on the performance of a multi-inlet gas cyclone. *Powder Technology, 384*, pp.82-99. https://doi.org/10.1016/j.powtec.2021.02.008.

[22] Dehdarinejad, E., Bayareh, M. and Ashrafizaadeh, M., 2021. A numerical study on combined baffles quick-separation device. International *Journal of Chemical Reactor Engineering, 19(5)*, pp.515-526.

https://doi.org/10.1515/ijcre-2021-0007.

[23] Dehdarinejad, E., Bayareh, M. and Ashrafizaadeh, M., 2022. Impact of cone wall roughness on turbulence swirling flow in a cyclone separator. *Chemical Papers*, 76(9), pp. 5579-5599. https://doi.org/10.1007/s11696-022-02261-6.

[24] Bayareh, M. and Dehdarinejad, E., 2022. Impact of Baffle and Cone Roughness on the Performance of a Solid-gas Separator Cyclone. In *41st ISTANBUL International Conference on Advances in Science, Engineering & Technology (IASET-22),* pp. 94–100. https://doi.org/10.17758/dirpub11.dir0522123.

[25] Kumar, M., Prakash, O. and Brar, L.S., 2025. Analyzing the impact of inclined single and multi-inlet configurations on the turbulent flow field in cyclone separators using large-eddy simulation. *Separation and Purification Technology,* p.134111. https://doi.org/10.1016/j.seppur.2025.134111.

[26] Vivek, R., Venkatesh, S. and Babu, K.S., 2025. Investigation on flow pattern and performance of square and cylindrical cyclone by experimental and numerical approach. *Powder Technology,* p.121427. https://doi.org/10.1016/j.powtec.2025.121427.

[27] Dehdarinejad, E. and Bayareh, M., 2022. Performance improvement of a cyclone separator using spiral guide vanes with variable pitch length. *Journal of the Brazilian Society of Mechanical Sciences and Engineering, 44(11),* p.516. https://doi.org/10.1007/s40430-022-03788-1.

[28] Dehdarinejad, E. and Bayareh, M., 2023. Analysis of the vortical flow in a cyclone using four vortex identification methods. *Powder Technology, 428,* p.118897. https://doi.org/10.1016/j.powtec.2023.118897.

[29] Dehdarinejad, E. and Bayareh, M., 2023. Experimental and numerical investigation on the performance of a gas-solid cyclone with twisted baffles and roughened cone surface. *Powder Technology, 420,* p.118401. https://doi.org/10.1016/j.powtec.2023.118401.

[30] Dehdarinejad, E. and Bayareh, M., 2021. An overview of numerical simulations on gas-solid cyclone separators with tangential inlet. *ChemBioEng Reviews, 8(4),* pp.375-391. https://doi.org/10.1002/cben.202000034.

[31] Dehdarinejad, E. and Bayareh, M., 2023. Performance analysis of a novel cyclone separator using RBFNN and MOPSO algorithms. *Powder Technology, 426,* p.118663. https://doi.org/10.1016/j.powtec.2023.118663.

[32] Dehdarinejad, E. and Bayareh, M., 2023. Effect of a new pattern of surface roughness on flow field and erosion rate of a cyclone. *International Journal of Chemical Reactor Engineering, 21(2),* pp.153-167. https://doi.org/10.1515/ijcre-2022-0064.

[33] Dehdarinejad, E. and Bayareh, M., 2022. Impact of non-uniform surface roughness on the erosion rate and performance of a cyclone separator. *Chemical Engineering Science, 249,* p.117351. https://doi.org/10.1016/j.ces.2021.117351.

[34] Dehdarinejad, E., Bayareh, M. and Ashrafizaadeh, M., 2022. Impact of cone wall roughness on turbulence swirling flow in a cyclone separator. *Chemical Papers*, 76(9), pp.5579-5599. https://doi.org/10.1007/s11696-022-02261-6.

[35] Fu, S., Tao, L., Shen, Z., Xu, M., Yang, D., Hu, Y. and Zhou, F., 2025. Effects of helical guide vanes on droplet behavior and separation performance in cyclone separators. *Chemical Engineering and Processing-Process Intensification, 209,* p.110197. https://doi.org/10.1016/j.cep.2025.110197.

[36] Dai, R., Fu, S. and Yuan, H., 2024. Study on the wall film behavior and droplet catching performance of a micro cyclone in hydrogen fuel cells. *International Journal of Hydrogen Energy, 61,* pp.125-136. https://doi.org/10.1016/j.ijhydene.2024.02.183.

[37] Cao, G., Sun, G., Yuan, S. and Wu, Y., 2025. Study on the influence of spiral guide vanes on gas/particle flow characteristics in FCC cyclone separator. *Separation and Purification Technology, 353,* p.128352. https://doi.org/10.1016/j.seppur.2024.128352.

[38] Sun, Z., Yang, H., Zhang, K., Wang, Z., Hong, Z. and Yang, G., 2024. Self-cleaning effect and secondary swirling clean gas for suppressing particle deposition on vortex finder of gas cyclones. *Particuology, 90,* pp.72-87. https://doi.org/10.1016/j.partic.2023.11.021.

[39] Barua, S., Batcha, M.F.M., Mohammed, A.N., Saif, Y., Al-Alimi, S., Al-fakih, M.A. and Zhou, W., 2024. Numerical Investigation of Inlet Height and Width Variations on Separation Performance and Pressure Drop of Multi-Inlet Cyclone Separators. *Processes, 12(9),* p.1820. https://doi.org/10.3390/pr12091820.

[40] Madaliev, M., Abdulkhaev, Z., Khusanov, Y., Mirzababayeva, S. and Abobakirova, Z., 2024. Numerical study of highly efficient centrifugal cyclones. *Acta hydrotechnica, 37(67)*, pp.137-151. https://doi.org/10.15292/acta.hydro.2024.08.

[41] Samadi, M., Mesbah, M. and Majidi, S., 2024. A novel approach to designing compact cyclones for efficient natural gas filtration. *Powder Technology, 448*, p.120259. https://doi.org/10.1016/j.powtec.2024.120259.

[42] Tang, Y., Xie, N., He, Y., Zhou, Y., Li, Z. and Wang, G., 2024. Study on the performance of downhole spiral-cyclone coupling separator for natural gas hydrate. *Advanced Powder Technology, 35(10),* p.104638. https://doi.org/10.1016/j.apt.2024.104638.

[43] Sun, Z., Yang, H., Zhang, K., Yan, Z., Su, N., Li, K. and Yang, G., 2024. 3D-printed elliptical cyclone separator with additional self-excited force field for enhancing the gas-solid separation. *Advanced Powder Technology, 35(7),* p.104496. https://doi.org/10.1016/j.apt.2024.104496.

[44] Zhao, J., Hao, X., Guo, X., Gao, F., Fan, J., Zhang, P. and Chen, G., 2025. Effect of local erosion on flow pattern and particle self-rotation in a cyclone separator. *Advanced Powder Technology, 36(7),* p.104949. https://doi.org/10.1016/j.apt.2025.104949.

[45] Liang, Y., Cheng, T., Li, Q., Liu, J., Li, Q., Li, J., Ma, S., Jiang, X., Wang, H. and Fu, P., 2024. CFD-DEM simulation of cyclone self-rotation drying: Particle high-speed self-rotation and heat transfer. *Energy, 290,* p.130277. https://doi.org/10.1016/j.energy.2024.130277.

[46] Hoffmann, A.C., Stein, L.E., 2008. Gas cyclones and swirl tubes: Principles, Des. Oper. 2nd Ed. Springer. https://doi.org/10.1007/978-3-540-74696-6.

[47] Griffiths, W.D. and Boysan, F., 1996. Computational fluid dynamics (CFD) and empirical modelling of the performance of a number of cyclone samplers. *Journal of Aerosol Science, 27(2),* pp. 281-304. https://doi.org/10.1016/0021-8502(95)00549-8.

[48] Bogodage, S.G. and Leung, A.Y.T., 2016. Improvements of the cyclone separator performance by down-comer tubes. *Journal of Hazardous Materials, 311*, pp.100-114. https://doi.org/10.1016/j.jhazmat.2016.02.072.

[49] Bogodage, S.G. and Leung, A.Y., 2015. CFD simulation of cyclone separators to reduce air pollution. *Powder Technology, 286,* pp.488-506. https://doi.org/10.1016/j.powtec.2015.08.023.

[50] Cortes, C. and Gil, A., 2007. Modeling the gas and particle flow inside cyclone separators. *Progress in energy and combustion Science, 33(5),* pp.409-452. https://doi.org/10.1016/j.pecs.2007.02.001.

[51] Zhao, B., 2005. Development of a new method for evaluating cyclone efficiency. *Chemical Engineering and Processing: Process Intensification, 44(4),* pp.447-451. https://doi.org/10.1016/j.cep.2004.06.007.

[52] Theodore, L. and Paola, V.D., 1980. Predicting cyclone efficiency. *Journal of the Air Pollution Control Association, 30(10),* pp.1132-1133. https://doi.org/10.1080/00022470.1980.10465160.

[53] Lapple, C.E., 1950. Gravity and centrifugal separation. *American Industrial Hygiene Association Quarterly, 11(1),* pp.40-48. https://doi.org/10.1080/00968205009344283.

[54] Dirgo, J. and Leith, D., 1985. Cyclone collection efficiency: comparison of experimental results with theoretical predictions. *Aerosol science and technology, 4(4),* pp.401-415. https://doi.org/10.1080/02786828508959066.

[55] Gimbun, J., Chuah, T.G., Choong, T.S. and FakhrúL-Razi, A., 2006. Evaluation on empirical models for the prediction of cyclone efficiency. *Journal-The institution of Engineers, Malaysia, 67(3),* pp.54-58. https://www.academia.edu/19574858/Evaluation_on_empirical_models_for_the_prediction_of_cyclone_efficiency.

[56] Xiang, R., Park, S.H. and Lee, K.W., 2001. Effects of cone dimension on cyclone performance. *Journal of Aerosol Science, 32(4),* pp.549-561. https://doi.org/10.1016/S0021-8502(00)00094-X.

[57] Leith, D. and Mehta, D., 1973. Cyclone performance and design. *Atmospheric Environment (1967), 7(5),* pp. 527-549. https://doi.org/10.1016/0004-6981(73)90006-1.

[58] Wan, G., Sun, G., Xue, X. and Shi, M., 2008. Solids concentration simulation of different size particles in a cyclone separator. *Powder technology, 183(1),* pp. 94-104. https://doi.org/10.1016/j.powtec.2007.11.019.

[59] Xue, X., Sun, G., Wan, G. and Shi, M., 2007. Numerical simulation of particle concentration in a gas cyclone separator. *Petroleum Science, 4(3),* pp. 76-83. https://doi.org/10.1007/s12182-007-0013-x.

[60] Mothe, H. and Loffler, F., 1988. Prediction of Particle Removal in Cyclone Separator. *International Journal of Chemical Engineering, 28,* pp. 231-240.

[61] Danckwerts, P.V., 1995. Continuous flow systems. Distribution of residence times. *Chemical engineering science, 50(24),* pp.3857-3866. https://doi.org/10.1016/0009-2509(96)81811-2.

[62] Iozia, D.L. and Leith, D., 1990. The logistic function and cyclone fractional efficiency. *Aerosol Science and Technology, 12(3),* pp. 598-606. https://doi.org/10.1080/02786829008959373.

[63] Kim, J.C. and Lee, K.W., 1990. Experimental study of particle collection by small cyclones. *Aerosol Science and Technology, 12(4),* pp. 1003-1015. https://doi.org/10.1080/02786829008959410.

[64] Clift, R., Ghadiri, M. and Hoffman, A.C., 1991. A critique of two models for cyclone performance. *AIChE Journal, 37(2),* pp. 285-289. https://doi.org/10.1002/aic.690370217.

[65] Muschelknautz, U. and Muschelknautz, E., 1999. Separation efficiency of recirculating cyclones in circulating fluidized bed combustions. *VGB PowerTech, 4,* p.99. https://www.mkengineering.de/english/pdf/VGBZWSEN.PDF.

[66] Muschelknautz, U. and Muschelknautz, E., 1999. Improvements of cyclones in CFB power plants and quantitative estimations of their effects on the boilers solids inventory. https://www.osti.gov/etdeweb/biblio/20054162.

[67] Hoffmann, A.C. and Stein, L.E., 2008. How cyclones work. In *Gas Cyclones and Swirl Tubes: Principles, Design and Operation* (pp. 37-48). Berlin, Heidelberg: Springer Berlin Heidelberg. https://doi.org/10.1007/978-3-540-74696-6.

[68] Hoffmannc, A.C., Van Santen, A., Allen, R.W.K. and Clift, R., 1992. Effects of geometry and solid loading on the performance of gas cyclones. *Powder Technology, 70(1),* pp. 83-91. https://doi.org/10.1016/0032-5910(92)85058-4.

[69] Dietz, P.W., 1981. Collection efficiency of cyclone separators. *AIChE Journal, 27(6),* pp. 888-892. https://doi.org/10.1002/aic.690270603.

[70] Patterson, P.A. and Munz, R.J., 1996. Gas and particle flow patterns in cyclones at room and elevated temperatures. *The Canadian Journal of Chemical Engineering, 74(2),* pp. 213-221. https://doi.org/10.1002/cjce.5450740206.

[71] Stairmand, C.J., 1951. The design and performance of cyclone separators. *Transactions of the Institution of Chemical Engineers, 29,* pp. 356-362. https://cir.nii.ac.jp/crid/1571698599847452416.

[72] Salcedo, R.L. and Coelho, M.A., 1999. Turbulent dispersion coefficients in cyclone flow: An empirical approach. *The Canadian Journal of Chemical Engineering, 77(4),* pp. 609-617. https://doi.org/10.1002/cjce.5450770401.

[73] Zhao, B., Wang, D., Su, Y. and Wang, H.L., 2020. Gas-particle cyclonic separation dynamics: modeling and characterization. *Separation & Purification Reviews, 49(2),* pp. 112-142. https://doi.org/10.1080/15422119.2018.1528278.

[74] Barth, W., 1956. Design and layout of the cyclone separator on the basis of new investigations. *Brenn. Warme Kraft, 8(1),* p.9.

[75] Enliang, L. and Yingmin, W., 1989. A new collection theory of cyclone separators. *AIChE Journal, 35(4),* pp. 666-669. https://doi.org/10.1002/aic.690350419.

[76] Ray, M.B., Hoffmann, A.C. and Postma, R.S., 2000. Performance of different analytical methods in evaluating grade efficiency of centrifugal separators. *Journal of aerosol science, 31(5),* pp. 563-581. https://doi.org/10.1016/S0021-8502(99)00543-1.

[77] Gil, A., Romeo, L.M. and Cortés, C., 2001. Cold

flow model of a PFBC cyclone. *Powder technology, 117(3),* pp. 207-220. https://doi.org/10.1016/S0032-5910(00)00371-5.

[78] Zhao, B.I.N.G.T.A.O., 2004. A theoretical approach to pressure drop across cyclone separators. *Chemical Engineering & Technology: Industrial Chemistry-Plant Equipment-Process Engineering-Biotechnology, 27(10),* pp. 1105-1108. https://doi.org/10.1002/ceat.200402089.

[79] McK, R., 1949. Fundamentals of cyclone design and operation. *Proceedings of the Australian Institute of Mining and Metallurgy, 152,* p.203. https://cir.nii.ac.jp/crid/1573668924879693312.

[80] Shephered, C.B. and Lapple, C.E., 1939. Flow pattern and pressure drop in cyclone dust collectors. *Industrial & Engineering Chemistry, 31(8),* pp.972-984. https://doi.org/10.1021/ie50356a012.

[81] Stairmand, C.J., 1949. Pressure drop in cyclone separators. *Engineering. 168,* p.409.

[82] Basu, P., 2006. Gas–Solid Separators. In *Combustion and Gasification in Fluidized Beds* (pp. 381-416). CRC Press. https://www.taylorfrancis.com/chapters/edit/10.1201/9781420005158-12/gas%E2%80%93solid-separators-prabir-basu.

[83] Ji, Z., Xiong, Z., Wu, X., Chen, H. and Wu, H., 2009. Experimental investigations on a cyclone separator performance at an extremely low particle concentration. *Powder Technology, 191(3),* pp. 254-259. https://doi.org/10.1016/j.powtec.2008.10.015.

[84] Casal, J. and JM, M.B., 1983. A better way to calculate cyclone pressure drop. http://pascal-francis.inist.fr/vibad/index.php?action=getRecordDetail&idt=PASCAL83X0128572.

[85] McK, R., 1949. Fundamentals of cyclone design and operation. *Proc. Aust. Inst. Mining Met., 152,* p. 203. https://cir.nii.ac.jp/crid/1573668924879693312.

[86] Belkner, J., Leineweber, J., Hein, G., Stauffenberg, J., Barth, A., Kissinger, T., Manske, E. and Fröhlich, T., 2025. An integrated exposure and measurement tool for 5-DOF direct laser writing based on chromatic differential confocal sensing. *Journal of the European Optical Society-Rapid Publications, 21(1),* p. 27. https://doi.org/10.1051/jeos/2025017.

[87] Kuo, K.Y. and Tsai, C.J., 2001. On the theory of particle cutoff diameter and collection efficiency of cyclones. *Aerosol and air quality research, 1(1),* pp. 47-56. https://doi.org/10.4209/aaqr.2001.06.0005.

[88] MOORE, M.E. and McFARLAND, A.R., 1990. Design of Stairmand-type sampling cyclones. *American Industrial Hygiene Association Journal, 51(3),* pp. 151-159. https://doi.org/10.1080/15298669091369475.

[89] Trefz, M. and Muschelknautz, E., 1993. Extended cyclone theory for gas flows with high solids concentrations. *Chemical Engineering & Technology: Industrial Chemistry-Plant Equipment-Process Engineering-Biotechnology, 16(3),* pp. 153-160. https://doi.org/10.1002/ceat.270160303.

[90] Gil, A., Romeo, L.M. and Cortes, C., 2002. Effect of the solid loading on a PFBC cyclone with pneumatic extraction of solids. *Chemical engineering & technology, 25(4),* pp.407-415. https://doi.org/10.1002/1521-4125(200204)25:4%3C407::AID-CEAT407%3E3.0.CO;2-4.

[91] Fassani, F.L. and Goldstein Jr, L., 2000. A study of the effect of high inlet solids loading on a cyclone separator pressure drop and collection efficiency. *Powder Technology, 107(1-2),* pp. 60-65. https://doi.org/10.1016/S0032-5910(99)00091-1.

[92] Kang, S.K., Kwon, T.W. and Kim, S.D., 1989. Hydrodynamic characteristics of cyclone reactors. *Powder technology, 58(3), pp. 211-220.* https://doi.org/10.1016/0032-5910(89)80116-0.

[93] Yuu, S., Jotaki, T., Tomita, Y. and Yoshida, K., 1978. The reduction of pressure drop due to dust loading in a conventional cyclone. *Chemical Engineering Science, 33(12),* pp. 1573-1580. https://doi.org/10.1016/0009-2509(78)85132-X.

[94] KIMURA, N., HASEGAWA, Z. and AKAMATSU, T., 1972. Dust collection characteristics of collectron. *Journal of the Research Association of Powder Technology, Japan, 9(6),* pp. 392-398. https://doi.org/10.4164/sptj1964.9.392.

[95] Ter Linden, A.J., 1949. Investigations into cyclone dust collectors. *Proceedings of the Institution of Mechanical Engineers, 160(1),*

pp. 233-251. https://doi.org/10.1243/PIME_PROC_1949_160_025_02.

[96] Alexander, R.M., 1988. Elastic mechanisms in animal movement. *The Cambridge University.* https://www.cambridge.org/tf/universitypress/subjects/life-sciences/zoology/elastic-mechanisms-animal-movement.

[97] Häfner, H., Riecher-Rössler, A., Hambrecht, M., Maurer, K., Meissner, S., Schmidtke, A., Fätkenheuer, B., Löffler, W. and van der Heiden, W., 1992. IRAOS: an instrument for the assessment of onset and early course of schizophrenia. *Schizophrenia research, 6(3),* pp. 209-223. https://doi.org/10.1016/0920-9964(92)90004-O.

[98] Derksen, J.J., Sundaresan, S. and Van den Akker, H.E.A., 2006. Simulation of mass-loading effects in gas–solid cyclone separators. *Powder technology, 163(1-2),* pp. 59-68. https://doi.org/10.1016/j.powtec.2006.01.006.

[99] Qian, F., Huang, Z., Chen, G. and Zhang, M., 2007. Numerical study of the separation characteristics in a cyclone of different inlet particle concentrations. *Computers & chemical engineering, 31(9),* pp. 1111-1122. https://doi.org/10.1016/j.compchemeng.2006.09.012.

[100] Hugi, E. and Reh, L., 2000. Focus on solids strand formation improves separation performance of highly loaded circulating fluidized bed recycle cyclones. *Chemical Engineering and Processing: Process Intensification, 39(3),* pp. 263-273. https://doi.org/10.1016/S0255-2701(99)00072-0.

[101] Hoffmann, A.C., De Jonge, R., Arends, H. and Hanrats, C., 1995. Evidence of the 'natural vortex length'and its effect on the separation efficiency of gas cyclones. *Filtration & Separation, 32(8),* pp. 799-804. https://doi.org/10.1016/S0015-1882(97)84131-6.

[102] Comas, M., Comas, J., Chetrit, C. and Casal, J., 1991. Cyclone pressure drop and efficiency with and without an inlet vane. *Powder technology, 66(2),* pp. 143-148. https://doi.org/10.1016/0032-5910(91)80095-Z.

[103] Hoffmann, A.C., Arends, H. and Sie, H., 1991. An experimental investigation elucidating the nature of the effect of solids loading on cyclone performance. *Filtration & separation, 28(3),* pp. 188-193. https://doi.org/10.1016/0015-1882(91)80074-F.

[104] Mothes, H. and Löffler, F., 1985. Motion and deposition of particles in cyclones. *German chemical engineering, 8(4),* pp. 223-233. http://pascal-francis.inist.fr/vibad/index.php?action=getRecordDetail&idt=9230220.

[105] Baskakov, A.P., Dolgov, V.N. and Goldobin, Y.M., 1990. Aerodynamics and heat transfer in cyclones with particle-laden gas flow. *Experimental Thermal and Fluid Science, 3(6),* pp. 597-602. https://doi.org/10.1016/0894-1777(90)90076-I.

[106] Huang, Y., Mo, X., Yang, H., Zhang, M. and Lv, J., 2016, July. Effects of Cyclone Structures on the Pressure Drop Across Different Sections in Cyclone Under Gas–Solid Flow. In *Clean Coal Technology and Sustainable Development: Proceedings of the 8th International Symposium on Coal Combustion* (pp. 301-307). Singapore: Springer Singapore. https://doi.org/10.1007/978-981-10-2023-0_40.

[107] El Ashry, Y., Abdelrazek, A.M. and Elshorbagy, K.A., 2018. Numerical and experimental study on the effect of solid particle sphericity on cyclone pressure drop. *Separation Science and Technology, 53(15),* pp. 2500-2516. https://doi.org/10.1080/01496395.2018.1458878.

[108] Hwang, I.S., Jeong, H.J. and Hwang, J., 2019. Numerical simulation of a dense flow cyclone using the kinetic theory of granular flow in a dense discrete phase model. *Powder Technology, 356,* pp. 129-138. https://doi.org/10.1016/j.powtec.2019.08.008.

[109] Li, S., Yang, H., Wu, Y.U.X.I.N. and Zhang, H., 2011. An Improved Cyclone Pressure Drop Model at High Inlet Solid Concentrations. *Chemical engineering & technology, 34(9),* pp. 1507-1513. https://doi.org/10.1002/ceat.201100087.

[110] Wu, X., Liu, J., Xu, X. and Xiao, Y., 2011. Modeling and experimental validation on pressure drop in a reverse-flow cyclone separator at high inlet solid loading. *Journal of Thermal Science, 20(4),* pp.343-348. https://doi.org/10.1007/s11630-011-0479-0.

[111] Nakhaei, M., Lu, B., Tian, Y., Wang, W., Dam-Johansen, K. and Wu, H., 2020. CFD modeling of gas–solid cyclone separators at ambient and elevated temperatures.

Processes, 8(2), p. 228. https://doi.org/10.3390/pr8020228.

[112] Dewil, R., Baeyens, J. and Caerts, B., 2008. CFB cyclones at high temperature: Operational results and design assessment. *Particuology, 6(3),* pp. 149-156. https://doi.org/10.1016/j.partic.2008.01.002.

[113] Bohnet, M., 1995. Influence of the gas temperature on the separation efficiency of aerocyclones. *Chemical Engineering and Processing: Process Intensification, 34(3),* pp. 151-156. https://doi.org/10.1016/0255-2701(94)04001-X.

[114] Patterson, P.A. and Munz, R.J., 1989. Cyclone collection efficiencies at very high temperatures. *The Canadian Journal of Chemical Engineering, 67(2),* pp. 321-328. https://doi.org/10.1002/cjce.5450670219.

[115] Gimbun, J., 2008. CFD simulation of aerocyclone hydrodynamics and performance at extreme temperature. *Engineering Applications of Computational Fluid Mechanics, 2(1),* pp. 22-29. https://doi.org/10.1080/19942060.2008.11015208.

[116] Rajan, K.S., Dhasandhan, K., Srivastava, S.N. and Pitchumani, B., 2008. Studies on gas–solid heat transfer during pneumatic conveying. *International Journal of Heat and Mass Transfer, 51(11-12)*, pp. 2801-2813. https://doi.org/10.1016/j.ijheatmasstransfer.2007.09.042.

[117] Szekely, J. and Carr, R., 1966. Heat transfer in a cyclone. *Chemical Engineering Science, 21(12),* pp. 1119-1132. https://doi.org/10.1016/0009-2509(66)85033-9.

[118] Danyluk, S., Shack, W.J., Park, J.Y. and Mamoun, M.M., 1980. The erosion of a type 310 stainless steel cyclone from a coal gasification pilot plant. *Wear, 63(1),* pp. 95-104. https://doi.org/10.1016/0043-1648(80)90076-9.

[119] McK, R., 1949. Fundamentals of cyclone design and operation. *Proceedings of the Australian Institute of Mining and Metallurgy, 152,* p. 203. https://cir.nii.ac.jp/crid/1573668924879693312.

[120] Bryant, H.S., Silverman, R.W. and Zenz, F.A., 1983. How dust in gas affects cyclone pressure drop. *Hydrocarbon Process.; (United States), 62(6)*.

[121] Mothes, H., 1988. Prediction removal in cyclone separators. *International Journal of Chemical Engineering, 28*, pp. 231–240.

[122] Ji, Z., Wu, X. and Shi, M., 1993. Experimental research on the natural turning length in the cyclone. *Acta Petrolei Sinica (Petroleum Processing Section), 9,* pp. 86-86.

[123] Hoffmann, A.C., De Groot, M., Peng, W., Dries, H.W.A. and Kater, J., 2001. Advantages and risks in increasing cyclone separator length. *AIChE journal, 47(11),* pp. 2452-2460. https://doi.org/10.1002/aic.690471109.

[124] Qian, F. and Zhang, M., 2005. Study of the natural vortex length of a cyclone with response surface methodology. *Computers & chemical engineering, 29(10)*, pp. 2155-2162. https://doi.org/10.1016/j.compchemeng.2005.07.011.

[125] Maclean, P., Brown, J.D., Hoy, H.D., Cantwell, J.E., 1978. UK patent application GB 2011285A, United Kingdom.

[126] Li, X., Song, J., Sun, G., Jia, M., Yan, C., Yang, Z. and Wei, Y., 2016. Experimental study on natural vortex length in a cyclone separator. *The Canadian Journal of Chemical Engineering, 94(12),* pp. 2373-2379. https://doi.org/10.1002/cjce.22598.